Environment International 195 (2025) 109207

Contents lists available at ScienceDirect

Environment International

journal homepage: www.elsevier.com/locate/envint

Full length article

Response of South Asia $PM_{2.5}$ pollution to ammonia emission changes and associated impacts on human health

Yuanlin Wang [a,*], Eiko Nemitz [a], Samuel J. Tomlinson [b], Edward J. Carnell [a], Liquan Yao [a,c,d], Janice Scheffler [a], Tomas Liska [a], Clare Pearson [a], Ulrike Dragosits [a], Chandra Venkataraman [e,f], Srinidhi Balasubramanian [f,g], Rachel Beck [a], Mark A. Sutton [a], Massimo Vieno [a]

[a] UK Centre for Ecology & Hydrology Edinburgh, Bush Estate, Penicuik EH26 0QB, UK
[b] UK Centre for Ecology & Hydrology Lancaster, Bailrigg, Lancaster Environment Centre, LA1 4AP, UK
[c] Department of Environmental Science, School of Resource and Environment, Henan Institute of Science and Technology, Xinxiang 453003, China
[d] Department of Atmospheric Sciences, School of Environmental Studies, China University of Geosciences, Wuhan 430074, China
[e] Department of Chemical Engineering, Indian Institute of Technology Bombay, Powai, Mumbai, India
[f] Center for Climate Studies, Indian Institute of Technology Bombay, Powai, Mumbai, India
[g] Environmental Science and Engineering Department, Indian Institute of Technology Bombay, Powai, Mumbai, India

ARTICLE INFO

Keywords:
$PM_{2.5}$
NH_3 emissions changes
Air pollution
Health impacts
Economic losses

ABSTRACT

Countries in South Asia are suffering severe $PM_{2.5}$ pollution with rapid economic development, impacting human health and the environment. Whilst much attention has been given to understanding the contribution of primary emissions, the contribution of agriculture to $PM_{2.5}$ concentrations, especially from agricultural ammonia (NH_3) emissions, remains less explored. Using an advanced regional atmospheric chemistry and transport modelling system (WRF-EMEP) with a new estimate of anthropogenic NH_3 emissions inputs, we estimate the influence of agricultural NH_3 emissions on surface $PM_{2.5}$ in South Asia and evaluate the health impacts and the economic losses attributable to $PM_{2.5}$ in 2018. Results show that WRF-EMEP can reproduce magnitudes and variations of $PM_{2.5}$ well, with a high annual mean $PM_{2.5}$ concentration that exceeds 120 μg/m^2 and mainly appeared in the Indo-Gangetic Plain. We estimate 2,228,000 (95 % Confidence Interval: 2,052,000–2,400,000) premature deaths and US$ 596,000 (95 % CI: 549,000–642,000) million in economic losses are attributable to total ambient $PM_{2.5}$ under the current emissions. We calculate that NH_3 emissions are associated with 11 % of the annual average $PM_{2.5}$ concentrations across South Asia. Changes in $PM_{2.5}$ concentrations follow a non-linear response to NH_3 emissions reductions, highlighting increased efficiency with 70 %–100 % reductions in NH_3 emissions reductions. We estimate that 247,000 (227,000–265,000) premature deaths and US$ 66,000 (61,000–71,000) million economic losses through this pathway can be attributed to NH_3 emissions. These findings confirm that in the current NH_3-rich chemical environment of South Asia, the efficiency of $PM_{2.5}$ reduction is only moderately sensitive to the reduction in intensity of NH_3 emissions until emissions are cut very severely. Thus, SO_2, NO_x and NH_3 emissions controls need to be considered jointly for greater mitigation of ambient secondary $PM_{2.5}$ in South Asia.

1. Introduction

With the rapid development of industries and an expanding population, countries in South Asia are experiencing severe air pollution. The World Health Organization has reported that 16 cities in South Asia rank among the top 20 most polluted globally (WHO, 2018). As one of the major components of air pollution, observed $PM_{2.5}$ (particles with an aerodynamic diameter less than 2.5 μm) concentrations were found to be 6–20 times higher than the WHO Air Quality Guidelines of 5 μg/m^3 in most South Asian cities (World Bank, 2023). Exposure to high concentrations of $PM_{2.5}$ has been linked to significant adverse effects on human health, including an increased risk of cardiovascular diseases, respiratory disease, and lung cancer (Cohen et al., 2017; Pope III et al., 2019; Coleman et al., 2020). The 2019 Global Burden of Disease Study (GBD 2019) identified ambient $PM_{2.5}$ pollution as the seventh greatest risk factor for all ages, attributing 4.1 million deaths to it globally (Sang

* Corresponding author at: UKCEH Centre for Ecology & Hydrology, Bush Estate, Penicuik, Midlothian EH26 0QB, UK.
E-mail address: yuawan@ceh.ac.uk (Y. Wang).

https://doi.org/10.1016/j.envint.2024.109207
Received 3 August 2024; Received in revised form 8 December 2024; Accepted 12 December 2024
Available online 16 December 2024
0160-4120/© 2024 The Author(s). Published by Elsevier Ltd. This is an open access article under the CC BY license (http://creativecommons.org/licenses/by/4.0/).

et al., 2022), including 0.98 million deaths in India alone (Pandey et al., 2021). Although some mitigation policies have been implemented in South Asian countries (e.g., India), reductions in $PM_{2.5}$ concentrations have not been effectively achieved (Chowdhury et al., 2017), and $PM_{2.5}$ pollution is expected to deteriorate in the coming decades due to rapid industrialization and urbanization. Furthermore, the high levels of $PM_{2.5}$ pollution in South Asia transported by the Asian summer monsoon also affect global climate and air quality (Lelieveld et al., 2018; Chen et al., 2020). $PM_{2.5}$ also affects ecosystems with chemical component species, contributing to the transport and deposition of eutrophying (nitrogen) compounds and acidity (Liu et al., 2019).

Atmospheric NH_3 is the only alkaline gas and plays a critical role between the atmosphere and biosphere (Chang et al., 1989; Sutton et al., 1993). NH_3 reacts with H_2SO_4, HNO_3 (formed by oxidation of SO_2 and NO_x, respectively (Hewitt, 2001)) and HCl to generate $(NH_4)_2SO_4$, NH_4HSO_4, NH_4NO_3 and NH_4Cl which are main constituents of $PM_{2.5}$. Studies reported secondary inorganic aerosols (SIA) that include sulfate, nitrate, chloride, and ammonium accounted for 25–75 % of $PM_{2.5}$ mass (Gray et al., 1986; Heitzenberg, 1989). In addition to reacting with acid gases, dry deposition and wet scavenging of NH_3 and ammonium contribute to the eutrophication of water bodies and acidification of terrestrial ecosystems (Zhang et al., 2010; Sheppard et al., 2011; Paerl et al., 2014). South Asia is one of the biggest hotspots of atmospheric NH_3 as a globally leading grain producer with intensive agricultural activities and fertilizer applications (Pawar et al., 2020; Balasubramanian et al., 2020), especially in the Indo-Gangetic Plain (IGP). The IGP records the highest global NH_3 column concentrations ($> 6 \times 10^6$ mol/cm^2), as observed by satellite (Van Damme et al., 2014; Van Damme et al., 2018; Kuttippurath et al., 2020). Despite this, many mitigation policies in South Asian countries primarily focus on reducing SO_2 and NO_x emissions, but neglect NH_3 emissions, which can cause an increase in atmospheric NH_3 concentrations (Warner et al., 2017; Liu et al., 2018). Previous studies based on atmospheric modelling found that abating NH_3 emissions is more cost-effective for mitigating $PM_{2.5}$ pollution than nitrogen oxide control (Gu et al., 2021), and significantly decreases secondary inorganic aerosols levels e.g. in China (Xu et al., 2019; Han et al., 2020; Liu et al., 2021). Source attributions have often lumped together the impact of agricultural activity through residue burning and NH_3 emissions. For example, recently study (Chatterjee et al., 2023) has attributed 9 % of South Asia's $PM_{2.5}$ burden to agriculture, while Pozzer et al., (2017) investigated that 16 % of $PM_{2.5}$ in South Asia was attributable to agricultural emissions.

Accurate data on NH_3 emissions are crucial for quantifying the total NH_3 concentrations and understanding their impacts on $PM_{2.5}$ air pollution. Different global or regional emission datasets have been utilized in previous studies that focused on South Asia (Wang et al., 2020; Gu et al., 2021). The Emissions Database for Global Atmospheric Research (EDGAR) represents global anthropogenic emissions, compiling international statistics with a consistent methodology. It includes agricultural activity data for NH_3 emissions sourced from the Food and Agricultural Organization (FAO) (Crippa et al., 2018). The Hemispheric Transport of Air Pollution (HTAP) dataset was developed as a global mosaic of emissions, collecting officially reported data from various regions and countries and stitching them together. For countries without official data, or data missing from official reporting, HTAP uses the EDGAR emissions database (Crippa et al., 2023). The Regional Emission Inventory in Asia (REAS) has been included in the HTAP framework for South Asia specifically, offering a resolution of $0.25^\circ \times 0.25^\circ$ with monthly variations for the years 2000–2008, considering major NH_3 sources like livestock and fertilizer application (Kurokawa et al., 2013). Additionally, another inventory, the MIX dataset, also addresses Asian anthropogenic emissions (Li et al., 2017), with REAS being specifically applied to NH_3 emissions in South Asia. These NH_3 emissions inventories are instrumental in analyzing the NH_3 mass load across South Asia. However, significant socio-economic changes such as urbanization and industrialization, population migration, and increased fertilizer application have altered the intensity and distribution of NH_3 emissions in this region over the past decade. Consequently, it is essential to have an up-to-date and reliable emission inventory to accurately assess air pollution levels in South Asia, especially for the regional health impacts.

Premature mortality attributable to long-term exposure to ambient $PM_{2.5}$ has been assessed in individual South Asian countries in previous studies based on ground measurement, satellite retrievals, and model simulation (van Donkelaar et al., 2015; Cohen et al., 2017; Pandey et al., 2021; Maji et al., 2023; Chatterjee et al., 2023). Chowdhury and Dey (2016) reported an estimated 486,000 premature deaths in India, based on bias-corrected satellite-based $PM_{2.5}$ data. High-resolution atmospheric chemical models have enabled more detailed analyses, attributing specific emission sources to premature deaths. Lelieveld et al. (2015) attributed 645,000 deaths in India in 2010 to ambient $PM_{2.5}$, with residential energy and power generation being the primary sources, whereas agricultural NH_3 emissions contributed to only 1 %. Conibear et al. (2018) calculated 990,000 premature mortalities in India in 2016 to $PM_{2.5}$, with 52 % resulting from residential energy use. Different exposure–response functions have been applied for estimating $PM_{2.5}$-attributable premature mortality. The above studies rely on the Integrated Exposure-Response (IER) model (Burnett et al., 2014), which introduces uncertainties in highly polluted regions because the IER function incorporates data on $PM_{2.5}$-mortality associations from non-ambient $PM_{2.5}$ sources at elevated concentrations. To reduce these uncertainties, Burnett et al. (2018) developed a new global exposure mortality model (GEMM), which has been proven to improve accuracy for highly air polluted areas (Lelieveld et al., 2020). Currently, insufficient evidence exists with regard to the differential toxicity of the different $PM_{2.5}$ chemical components and we discuss associated uncertainties. In addition, previous studies relied on old emission inventories, which have since been updated. Furthermore, few studies have quantified the health impacts of $PM_{2.5}$ reduction through NH_3 emission changes. Notably, many studies have focused on individual countries (e.g. Ravishankara et al., 2020; Islam et al., 2023), without providing a comprehensive view of $PM_{2.5}$ pollution and associated health impacts across the whole South Asian region.

In this study, we employ a state-of-the-art atmospheric chemistry transport model (EMEP model), with an updated South Asia emission inventory specific to South Asia, to address the above challenges. The EMEP model using the gas/aerosol thermodynamic scheme EQSAM4-clim, has a low cost with respect to the total CPU consumption across aerosols with a range of composition complexity (Metzger et al., 2024), which makes it suitable for full-year scenario simulations at relatively high spatial resolution (Angelbratt et al., 2011; Simpson et al., 2014; Dong et al., 2018; Thunis et al., 2021). We perform a range of model simulations to evaluate the response of $PM_{2.5}$ pollution to global NH_3 reduction at various levels. We then quantify the premature human mortality in South Asia attributable to ambient $PM_{2.5}$, following NH_3 emissions reductions utilizing a newly updated concentration–response model. Additionally, economic losses related to health impacts due to $PM_{2.5}$ exposure are also assessed. The findings from this study provide crucial insights into the potential benefits of targeted NH_3 emissions control strategies, offering a scientific foundation for the development and implementation of more effective air pollution control policies in South Asia.

2. Methodology

2.1. The EMEP model

2.1.1. Introduction to the EMEP model

The model of the European Monitoring and Evaluation Programme Meteorological Synthesizing Centre-West (EMEP MSC-W) rv4.45 is applied in this study to generate concentrations of air pollutants (https://github.com/metno/emep-ctm/releases/tag/rv4_45, last access: 09

February 2024). This open-source 3-D Eulerian atmospheric chemical transport model has been widely used for scientific research and policy support on both global and regional scales (Vieno et al., 2016; Ge et al., 2021, 2023; Gu et al., 2021). The EMEP model includes a complete description of advection, diffusion, chemical reactions, and dry and wet deposition processes. It uses the Emchem19 chemical mechanism which includes ~ 75 chemical species, 140 chemical reactions, and 34 photodissociation reactions (Simpson et al., 2020) to calculate gas-phase chemistry. The aerosol thermodynamic scheme, Equilibrium Simplified Aerosol Model V4 (EQSAM4clim) is applied here to calculate gas/aerosol partitioning as it results in faster run times making it suitable for full-year scenario runs (Metzger et al., 2016, 2018). The parameterization of Wesely (1989) is used for dry deposition for most compounds, with an extended parameterization for some compounds including NH_3, SO_2 and O_3 (Simpson et al., 2012). Wet deposition processes are based on the parameterization of Berge and Jakobsen (1998). The volatility basis set (VBS) approach is added to simulated secondary organic aerosol dynamics (Robinson et al., 2007; Donahue et al., 2009; Bergstrom et al., 2012; Ots et al., 2016a, 2016b, 2018). A more technical description of the EMEP model rv4.0 is presented in Simpson et al. (2012), and an overview of model updates from version rv4.0 to rv4.45 is presented in Hilde et al. (2022).

2.1.2. Model configuration

The configuration of the model with two domains in the current study is shown in Fig. S1. The outer domain covers the globe at a horizontal resolution of 1° (360 x 180 grid cells), approximate 110 km at the equator. The inner domain covers South Asia (9° S – 41° N and 54° E – 104° E), at 0.11° (450 x 450 grid cells), around 12 km at the equator. Vertically, the EMEP model employs 21 terrain-following layers from the surface to 100 hPa, with the height of the lowest layer ~ 45 m. An intermediate model domain is used for the meteorology with a horizontal resolution of 0.33° (not shown here).

Meteorological fields used for the EMEP model in this study are calculated using the Weather Research and Forecasting (WRF) model v4.4.2 (Skamarock et al., 2019). The fifth-generation European Centre for Medium-Range Weather Forecasts (ECMWF) atmospheric reanalysis of the global climate (ERA5) at 0.25° resolution is used as a boundary condition. The wind speed, wind direction, specific humidity, and temperature were also nudged towards the ERA5 every 6 h. Within WRF, the current study applies the bulk microphysical parameterization scheme (Lin et al., 2011), the Rapid Radiative Transfer Model long-wave radiation scheme (Mlawer et al., 1997), the Dudhia short-wave radiation scheme (Dudhia et al., 1989), the Kain-Fritsch cumulus parameterization scheme (JS Kain et al., 2004) and the Yonsei University planetary boundary layer scheme (Hong et al., 2006). The Noah Land Surface Model (Chen and Dudhia 2001) is used in this WRF simulation. For land cover data we applied the Moderate Resolution Imaging Spectroradiometer (MODIS) products (https://modis.gsfc.nasa.gov/data/dataprod/mod12.php).

2.1.3. Emissions

The anthropogenic emissions used in the EMEP model are based upon the EDGARv6.1, for the year 2015 (Crippa et al., 2019; Janssens-Maenhout et al., 2019), with the exception that emissions of agricultural NH_3 (i.e. agricultural soils and manure management) for South Asian countries (Afghanistan, Bangladesh, Bhutan, India, Maldives, Nepal, Pakistan and Sri Lanka) were re-calculated using a bottom-up approach similar to Crippa et al. (2019) and Janssens-Maenhout et al. (2019), but with updated spatial proxies (e.g. Gridded Livestock of the World [GLW] version 4, plus more detailed crop surfaces) and sub-national activity data where available (Tomlinson et al., 2024). Furthermore, for India only, emissions of non-NH_3 air pollutants in India (NO_x, SO_2, CO, NMVOCs and $PM_{2.5}$) were replaced with a national inventory (Venkataraman et al., 2018; Sadavarte & Venkataraman, 2014; Pandey et al., 2014). This dataset uses consistent assumptions to calculate emissions of the suite of pollutants, including all sectors covered by global inventories, as well as agricultural residue burning emissions and industrial process emissions, whilst providing for finer spatial resolution using district-level data and sector-based spatial proxies. Fig. 1 shows the proportions of different emission sectors and the spatial distribution of NH_3 emissions in South Asia (those of other pollutants can be found in Fig. S2). The majority of NH_3 is emitted in India, Pakistan and Bangladesh, particularly along the IGP. Our estimate of annual NH_3 emissions in the study area is 8,905 kt, to which the agriculture sector contributes the biggest proportion (83 %). This is comparable to the 9,301 kt of NH_3 emissions estimated for the same countries in EDGARv6.1, but spatial and seasonal patterns are markedly different.

2.1.4. Model extension to chloride

Given the growing evidence that a significant fraction of ammonium in South Asian cities is present in the form of ammonium chloride (e.g. Gunthe et al., 2021), the standard EMEP model was here extended to include treatment of hydrogen chloride (HCl) and particulate chloride, similar to the approach Pawar et al. (2023) took for the WRF-Chem model. This included reading in global emissions of total chloride (Zhang et al., 2022) as HCl, deposition treatment analogous to nitric acid and fine aerosol nitrate, and activation of the thermodynamic treatment already implemented in the EQSAM4clim module. Biomass burning emissions were taken from the Fire Inventory from NCAR version 1.5 (Wiedinmyer et al., 2011). VOCs emissions from biogenic sources are calculated in the model based on meteorological conditions and land cover. Details of other emissions, i.e., aircraft, soil NO and lightning are described in Simpson et al (2012).

2.2. Observations and statistical metrics

Substantial observed data were collated and used to evaluate the performance of the WRF-EMEP model. Meteorological observations at 297 sites across South Asia in 2018 were obtained from the National Climatic Data Centre (https://ncdc.noaa.gov/isd/data-access), including temperature (Temp), relative humidity (RH), and wind speed (WS). Observations of hourly surface $PM_{2.5}$ concentrations for India in 2018 were collected from the Central Pollution Control Board (https://cpcb.nic.in). As we did not find national observations in other South Asian countries, hourly observed $PM_{2.5}$ data for Nepal, Bangladesh, and Sri Lanka were obtained from the US Embassies and consulates (https://www.airnow.gov/international/us-embassies-and-consulates). The $PM_{2.5}$ as calculated by the EMEP model is defined as particulate matter with aerodynamic diameter up to 2.5 μm. The modelled $PM_{2.5}$ refers to the sum of all aerosol species included in the EMEP model: sulfate, fine nitrate, ammonium, chloride, fine elemental carbon, fine secondary organic aerosols, fine sea salt, fine dust, primary $PM_{2.5}$ and 16 % of coarse nitrate, where fine and coarse present 2.5 μm and 2.5–10 μm particle size, respectively. Secondary inorganic aerosols include sulfate, fine nitrate, ammonium, and chloride (Simpson et al., 2012).

Statistical metrics such as mean bias (MB), normalized mean bias (NMB), root mean square error (RMSE), and correlation coefficient (R) are used to assess model performances. Additionally, we applied mean fractional bias (MFB) and mean fractional error (MFE) specifically for $PM_{2.5}$ evaluation (Boylan and Russell, 2006), which are calculated using Equations (1)-(2).

$$MFB = \frac{1}{N}\sum_{i=1}^{N}\frac{(C_m - C_o)}{\left(\frac{C_m + C_o}{2}\right)} \quad (1)$$

$$MFE = \frac{1}{N}\sum_{i=1}^{N}\frac{|C_m - C_o|}{\left(\frac{C_m + C_o}{2}\right)} \quad (2)$$

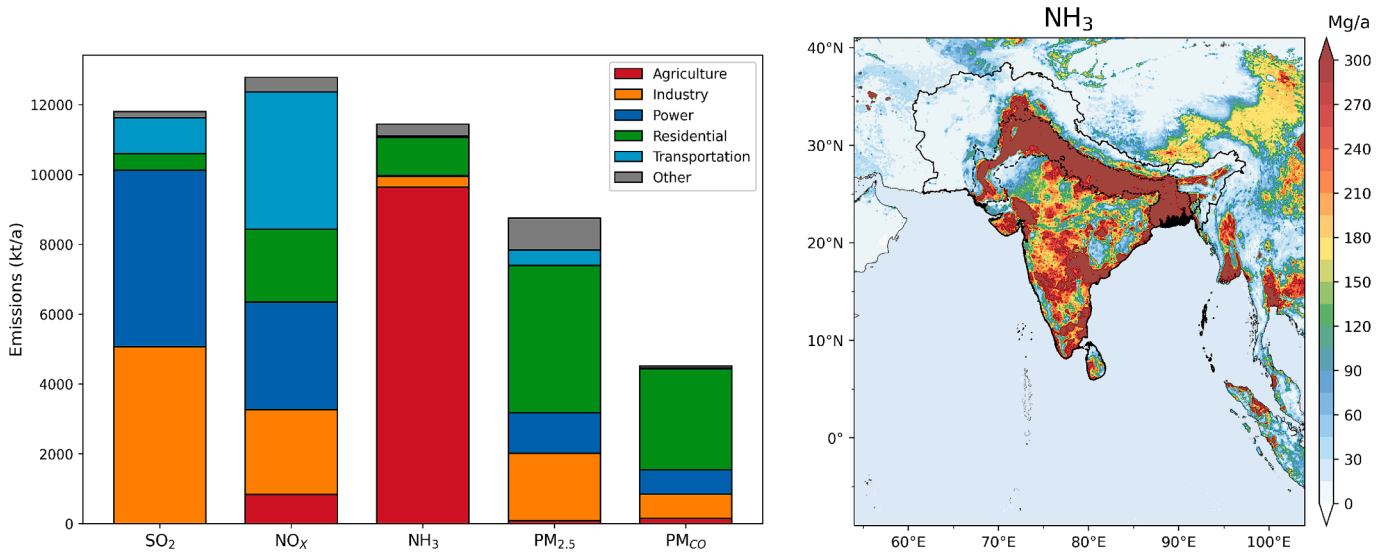

Fig. 1. The contributions of different emission sectors (left) and the spatial distribution of NH_3 emissions in South Asia (right). The solid line shows the outline of the South Asian countries and the dashed line represent the area of the Indo-Gangetic Plain (IGP), the IGP is defined as according to Agarwal et al (2024).

2.3. Assessing health impacts and economic valuation attributable to long-term $PM_{2.5}$ exposure

The Global Exposure Mortality Model (GEMM, Burnett et al., 2018) is used here to calculate the premature mortality attributable to long-term $PM_{2.5}$ exposure over South Asia in 2018. GEMM integrates data from 41 cohorts across 16 countries to generate the shape of the association between $PM_{2.5}$ and non-accidental mortality. Relying solely on outdoor $PM_{2.5}$ studies, GEMM covers much of the global exposure range compared to the older IER model (Burnett et al., 2014), including a study on a cohort of Chinese men that extended $PM_{2.5}$ concentration up to 84 μg/m^3. These updated functions have been widely applied in previous studies (see Milner et al., 2023; Maji K J et al., 2023; Zhang et al., 2019). In the current study, we apply GEMM to estimate health impacts related to total non-accidental mortality, which includes non-communicable disease (NCD) and lower respiratory infections (LRI), denoted as GEMM −NCD + LRI.

The relative risk (RR) is calculated as:

$$\Delta C = \max(0, C - C_0) \tag{3}$$

$$RR(\Delta C) = exp\left\{\frac{\theta \log(1 + \Delta C/\alpha)}{1 + \exp(-(\Delta C - \mu)/\nu)}\right\} \tag{4}$$

where Δ C is the excess of the annual average $PM_{2.5}$ concentration (C), over C_0 the counter-factual concentration ($C_0 = 2.4$ μg/m^3) below which no adverse health effects are observed, and α, μ, ν are fitting parameters that reproduce the observed concentration–response curves for different health endpoints and θ is estimated based on the Cox proportional hazards model (Cox, 1972). Mean relative risk and its 95 % confidence intervals (CIs) are calculated by a distribution of 1000 sets of parameters in the GEMM model. We assess $PM_{2.5}$-related mortality for adults at 5-year age intervals, starting from age 25 to ages greater than 80.

RR can be converted to premature mortality attributable to $PM_{2.5}$ exposure, for each endpoint for each age and sex subgroup in each country (subscripts *e, a, s, r*, respectively) over South Asia in 2018.

$$M_{e,a,s,r}(\Delta C) = Pop_{a,s,r} \times B_{e,a,s,r} \times \frac{RR_{e,a}(\Delta C) - 1}{RR_{e,a}(\Delta C)} \tag{5}$$

where $M_{e,a,s,r}$ is the $PM_{2.5}$-attributable premature mortality caused by a specific endpoint at a specific age, sex and country. $Pop_{a,s,r}$ represents the population exposed in a specific age-sex group at a country level. Population data at 1 km × 1 km resolution for 2018 was obtained from WorldPop (https://www.worldpop.org/) and re-gridded to 0.1° × 0.1° to match model resolution in the South Asian domain. $B_{e,a,s,r}$ represents the baseline mortality, i.e., the incidence of a specific health endpoint at a specific age-sex in a country. National baseline incidence rates of various health endpoints for different countries in South Asia were obtained from the Global Burden Disease (GBD) database (http://vizhub.healthdata.org/gbd-compare). To exclude the influence of population sizes between the different countries, we also calculate the per capita mortality by dividing the number of premature deaths by the population.

To calculate the fraction of $PM_{2.5}$ health impacts due to NH_3 emissions, we use the attribution and subtraction methods (Conibear et al., 2018; Gao et al., 2018). Philosophically, the attribution method and the subtraction method answer two different questions: the former quantifies the contribution of NH_3 as a component precursor for the $PM_{2.5}$ mix that is causing the current health impacts whilst the latter identifies the gains achievable by NH_3 emissions control given the currently high concentrations.

The approach computes fractional reduction in $PM_{2.5}$ concentration from reducing or removing anthropogenic NH_3 emissions globally, then applies this fraction to scale the overall estimate of premature mortality (Equation (4). In this study, we limit the assessment of the contributions of anthropogenic NH_3 emissions to the South Asian domain.

$$M_{NH_3} = M_{BASE} \times \frac{(PM_{2.5BASE} - PM_{2.5\_NH_3\_change})}{PM_{2.5BASE}} \tag{6}$$

The subtraction assesses the premature mortality due to NH_3 emissions (M_{NH_3}) by calculating the difference between the total premature mortality from all sources (M_{BASE}) and the premature mortality when anthropogenic NH_3 emissions are changed or removed (Equation (5).

$$M_{NH_3} = M_{BASE} - M_{NH_3\_change} \tag{7}$$

We further apply the Value of a Statistical Life (VSL) method to assess the economic losses of health impacts associated with $PM_{2.5}$ exposure in 2018 (Equation (5). VSL is the local trade-off rate between fatality risk and cost, indicating how much people would be willing to pay for a reduction (Gao et al., 2015). The unit economic costs of mortality for major countries in South Asia from Viscusi and Masterman (2017) are listed in Table 1:

$$E = C_p \times M \tag{8}$$

Table 1
Unit economic costs of mortality in South Asia (Viscusi and Masterman., 2017).

Countries	India	Pakistan	Nepal	Bangladesh	Sri Lanka	Bhutan	Afghanistan
Cost per case (US$)	275,000	248,000	126,000	205,000	654,000	409,000	105,000

where E is the economic losses of health impacts due to $PM_{2.5}$ concentrations, C_p is the cost per case and M is $PM_{2.5}$-attributable premature mortality estimated by attribution and subtraction approaches.

2.4. Sensitivity tests design

To evaluate the impacts of NH_3 emissions variations on $PM_{2.5}$ pollution and related health and economic losses, a series of simulations were here conducted for 2018. The baseline simulation (BASE) including all emissions mentioned above is compared with measurements. Other sensitivity simulations are implemented by reducing anthropogenic NH_3 emissions by 10 % steps (denoted as SN, N = 10, 20, 30…, 100).

3. Results

3.1. Model evaluation

Daily variations of observed and simulated major meteorological variables are is presented in Fig. S3. Simulations from the WRF model are overall in good agreement with observations from major countries in South Asia, particularly for temperature and relative humidity. It is worth noting that there is only one site in Bhutan; this is at an altitude above sea level of around 2200 m, while the grid average terrain height for that location in the WRF model is nearly 3000 m. The discrepancy in height explains the difference between the observed and modelled results, especially for temperature. The variations of observed wind speed are well reproduced by the model, but systematic overestimations were found in the simulations (by 0.1 to 1.8 m/s). Agarwal et al. (2023) used the WRF-Chem model and also observed this and suggested that it was driven by high nocturnal biases.

A comparison of observed and modelled daily mean $PM_{2.5}$ concentrations across four countries is shown in Fig. 2. The EMEP model can capture the magnitudes and temporal variations of observed $PM_{2.5}$ well, with R values greater than 0.4. The model performs very well in India, achieving a small MB of −7.6 μg/m^3 (NMB = -0.1) and a high R value of 0.8. Simulated $PM_{2.5}$ concentrations are underestimated in Bangladesh and Nepal during winter presumably due to accumulating or missing local emissions. Specifically in Nepal, both US sites located in Kathmandu observe substantial pollutants accumulation because of low windspeed and stagnant weather conditions, leading to elevated $PM_{2.5}$ concentrations. Conversely, the EMEP model slightly overestimates $PM_{2.5}$ in Sri Lanka during spring. We also provide a time series of observed and simulated daily mean $PM_{2.5}$ across 17 Indian cities (Fig. S4). Simulations compare reasonably well with observations in most cities, with R values greater than 0.5. Notably, the EMEP model accurately reproduces the magnitude and variation of observed $PM_{2.5}$ in Delhi, with an R value of 0.8 and MB value of −13 μg/m^3 (NMB = -0.1), even capturing peak winter concentrations. There are episodes where simulated concentrations are lower than observations, possibly due to adverse meteorological conditions.

Fig. 3 shows the $PM_{2.5}$ performance statistics of MFB and MFE as a function of absolute concentrations across all valid sites. There are various published performance criteria for air quality models. The U.S. EPA recommends a PM model performance goal of within ± 30 % for MFB and less than 50 % for MFE, and performance criteria of within ± 60 % for MFB and less than 75 % for MFE (U.S. EPA 2001). The "performance goal" represents the level of accuracy that is close to the best a model can be expected to achieve, and "criteria" indicates an acceptable level of accuracy (Boylan and Russell, 2006). Our $PM_{2.5}$ simulations meet the performance goal of MFB, with 23 % of values falling between the goal and criteria at most of sites. For MFE, 77 % of values are within the goal, with the rest are between the goal and criteria. Overall, EMEP model can provide confident and reliable $PM_{2.5}$ simulations compared to observations.

Fig. 4 displays the spatial distributions of the simulated annual mean $PM_{2.5}$, NH_3, and SIA for 2018, and their monthly spatial distributions can be found in Figs. S5 to S7. High $PM_{2.5}$ concentrations are mainly concentrated in the IGP and eastern India, exceeding 100 μg/m^3.

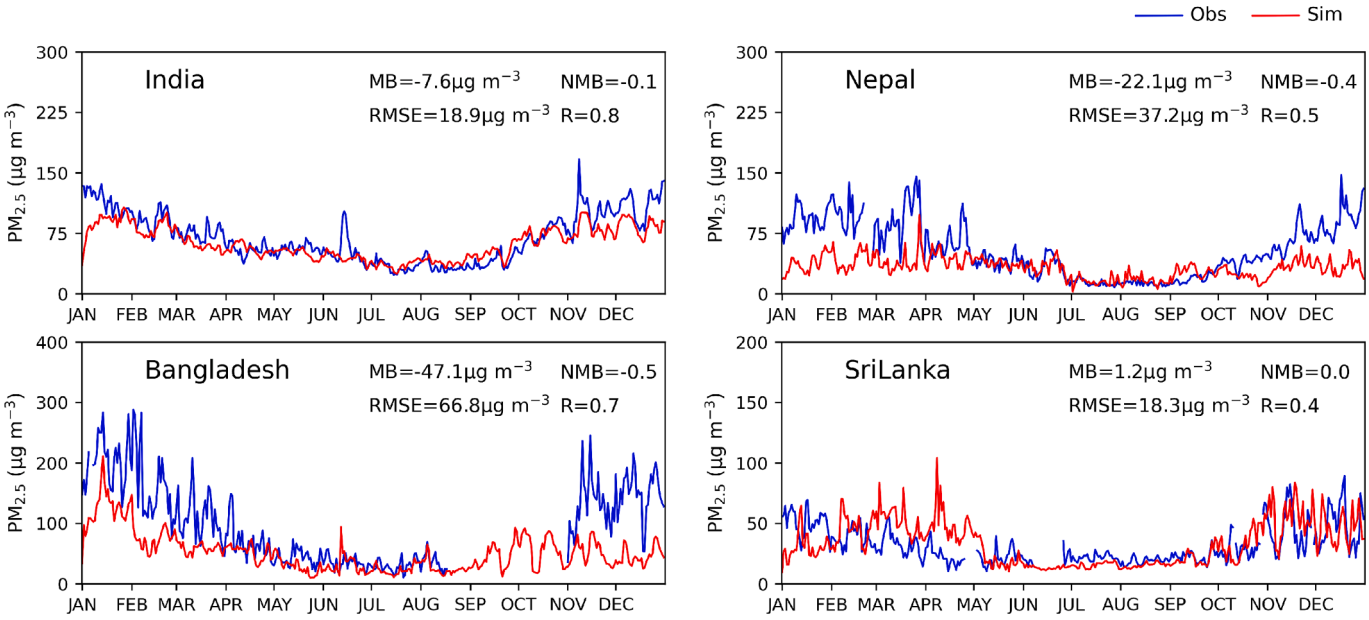

Fig. 2. Comparison of daily $PM_{2.5}$ concentrations between observations and simulations in four South Asian countries.

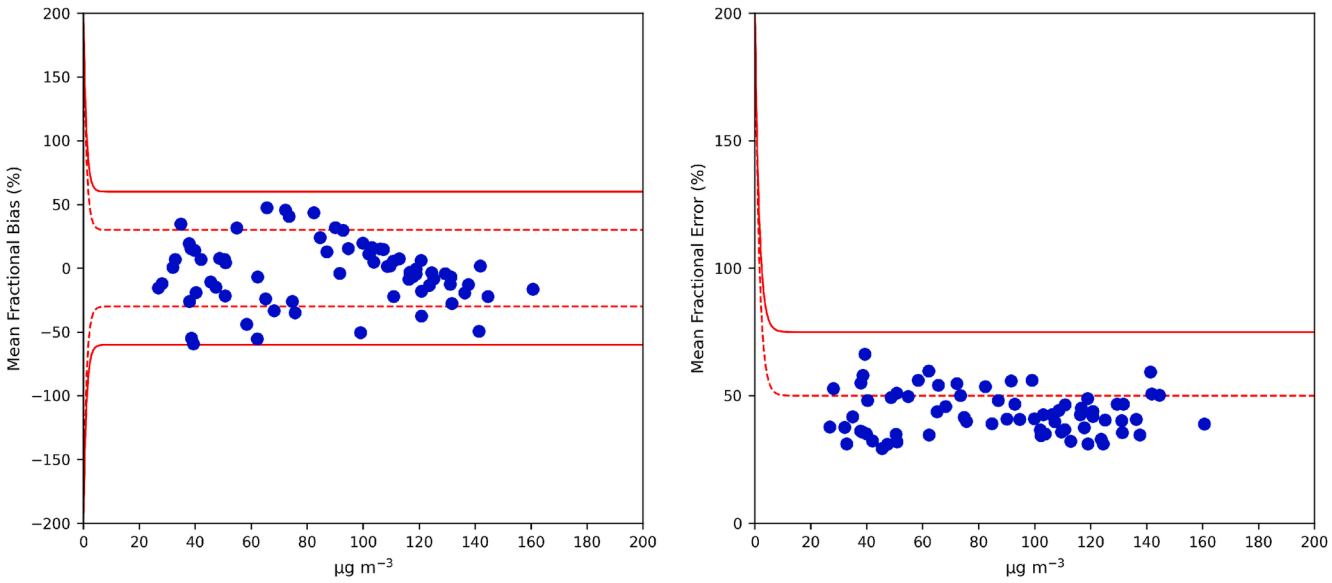

Fig. 3. Performance of simulated $PM_{2.5}$ concentrations. The x-axis shows the observations. The dashed line and solid line represent model performance goals and criteria, respectively.

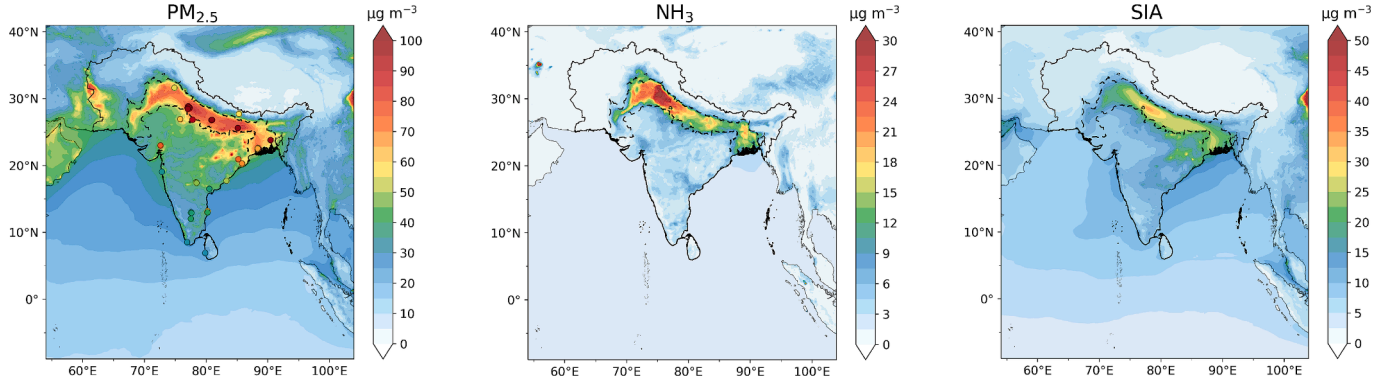

Fig. 4. Spatial distribution of annual simulated $PM_{2.5}$, NH_3, and SIA across South Asia (circles show annual mean observed values).

Because of increased emissions and unfavorable weather conditions, heavy $PM_{2.5}$ pollution are predicted to have occurred in winter with concentrations of more than 150 μg/m^3. Conversely, lower $PM_{2.5}$ concentrations (10 – 70 μg/m^3) were predicted for the monsoon season due to reduced SO_2, NO_x and primary emissions and increased wet deposition. In Delhi, the model underestimated $PM_{2.5}$. An increasing number of studies shows that in Delhi a substantial fraction of $PM_{2.5}$ is in particulate chloride form (Cash et al., 2020; Pawar et al., 2023). With the magnitude of HCl emissions in the first published emission inventory used here the EMEP model was not able to reproduce the measured levels of particulate Cl^-. This will have contributed to the underestimation of $PM_{2.5}$ in urban areas and will be the subject of future improvements. Annual NH_3 concentrations are over 30 μg/m^3 in the IGP. In contrast with the monthly variations of $PM_{2.5}$, NH_3 levels are predicted to peak in June, extending beyond the IGP to central India. Modelled NH_3 concentrations reach up to 40 μg/m^3 in Punjab and Haryana, India. Our results are in agreement with Kuttippurath et al. (2020), who reported high NH_3 total columns loading during the monsoon season because of high temperature, high agricultural activity levels and fertilizer applications by analyzing IASI satellite data. Based on WRF-Chem with satellite observations, Wang et al. (2020) identified that the reduced gas-to-particle conversion of NH_3 caused by low SO_2 and NO_x emissions also played an important role in high NH_3 concentrations loadings in monsoon season. Following the distribution patterns and temporal variations of $PM_{2.5}$, high SIA concentrations of around 25–35 μg/m^3 also occur in IGP.

3.2. *Impacts of NH_3 emissions reductions on $PM_{2.5}$ concentrations*

In the current study, ten sensitivity tests have been conducted to assess the response of air pollutants to NH_3 emissions reductions. Fig. 5 illustrates the changes in surface SIA and $PM_{2.5}$ concentrations between the BASE and the sensitivity runs due to NH_3 emissions reductions. The most notable changes in absolute terms happen in the IGP, where annual average SIA concentrations decrease by more than 15 μg/m^3 (40 %) when NH_3 emissions are reduced. This is also reflected in the predicted change in total $PM_{2.5}$ concentrations, which decline by more than 12 μg/m^3 (15 %) in most place of the IGP when NH_3 emissions are completely removed. Table 2 shows the relative change (%) of SIA and $PM_{2.5}$ concentrations in South Asian countries and the IGP resulting from NH_3 emissions reductions, comparing the BASE run with all sensitivity analyses. An annual reduction in NH_3 emissions by 10 % results in small decreases of 0.7 % in SIA and 0.2 % in $PM_{2.5}$ concentrations across South Asian countries, with slightly greater reductions observed in the IGP, where SIA and $PM_{2.5}$ concentrations drop by 1.1 % and 0.7 %, respectively. It is worth noting that the decrease in SIA and $PM_{2.5}$ mass burden accelerates with increasing NH_3 emissions reduction, e.g., a 100 % reduction in NH_3 emissions leads to a 32.3 % decrease in SIA and a 11.0

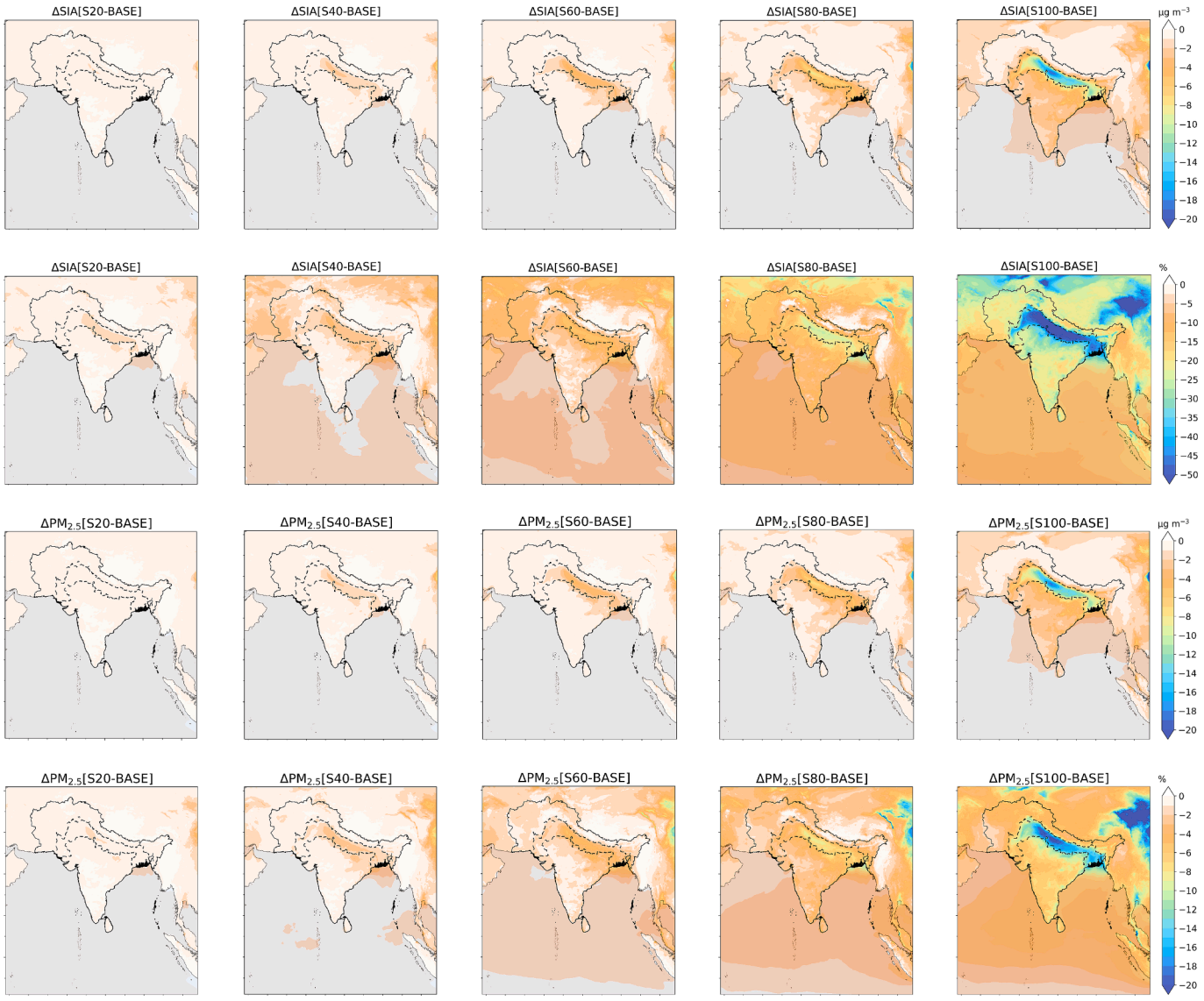

Fig. 5. The absolute and relative changes in annual average SIA and $PM_{2.5}$ concentrations between base and sensitivity runs with spatially homogeneous global NH_3 emissions reductions.

Table 2
The change percentage (%) of SIA and $PM_{2.5}$ concentrations between base and sensitivity runs with global NH_3 emissions reductions averaged over the South Asian countries and IGP.

	NH_3 emissions Reduction (%)	SA		IGP	
		SIA	$PM_{2.5}$	SIA	$PM_{2.5}$
S10-BASE	10	−0.7	−0.2	−1.1	−0.3
S20-BASE	20	−1.5	−0.4	−2.3	−0.7
S30-BASE	30	−2.4	−0.6	−3.7	−1.1
S40-BASE	40	−3.6	−0.9	−5.4	−1.6
S50-BASE	50	−5.2	−1.3	−7.4	−2.2
S60-BASE	60	−7.3	−1.9	−10.0	−2.9
S70-BASE	70	−10.2	−2.7	−13.6	−4.0
S80-BASE	80	−14.4	−3.8	−18.8	−5.6
S90-BASE	90	−21.0	−5.6	−27.8	−8.3
S100-BASE	100	−32.3	−11.0	−45.0	−13.6

% decline in $PM_{2.5}$ concentrations over South Asian countries, indicating a nonlinear response of PM pollution to changes in NH_3 emissions.

Fig. 6 shows the relative changes in annual mean concentrations of $PM_{2.5}$ and its components across different regions or countries in South Asia, driven by NH_3 emissions reductions in 2018 (with absolute variations shown in Fig. S8). Most species follow a non-linear response to NH_3 emissions reductions, except for chloride which demonstrates a nearly linear pattern. All trends become faster with increased NH_3 emissions reductions, particularly as the rate of change accelerating with reducing 70 %-100 % NH_3 emissions. Overall $PM_{2.5}$ and SIA concentrations decrease by 11.0 % and 32.3 % with NH_3 emissions removal across the South Asian region, respectively. As one of the most polluted areas, $PM_{2.5}$ and SIA decrease by 13.6 % (8.6 μg/m^3) and 45.1 % (8.9 μg/m^3) in the IGP. Among all South Asian countries, the largest decreases are observed for Bangladesh with a 14.2 % (7.7 μg/m^3) reduction in $PM_{2.5}$ and a 42.2 % (8.0 μg/m^3) reduction in SIA concentrations. Followed by India, where $PM_{2.5}$ and SIA concentrations decline by 9.8 % (4.1 μg/m^3) and 32.6 % (4.3 μg/m^3), respectively. Notably, $PM_{2.5}$ concentrations include 16 % of coarse nitrate, where a slight increase accounts for the minor discrepancies in absolute variations between $PM_{2.5}$ and SIA concentrations: reduced NH_3 emissions result in higher HNO_3 concentrations which in the model can then partition onto pre-existing coarse particles (dust and seasalt) (Simpson et al., 2012).

Because of the affinity of acidic gases for NH_3 and the more volatile

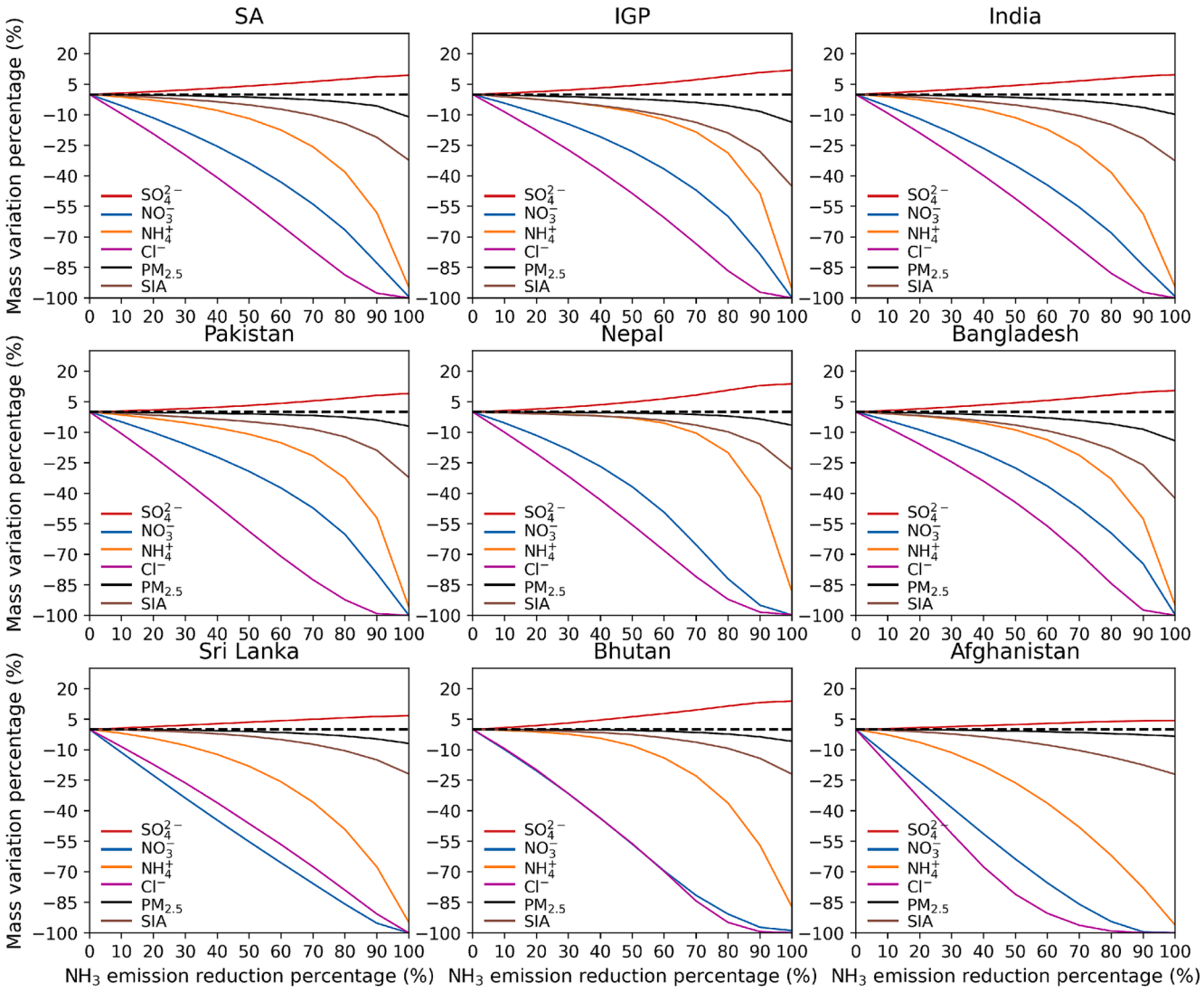

Fig. 6. The relative variations of aerosol concentrations associated with reduced NH_3 emissions (the dashed line represents zero mark).

nature of ammonium chloride, the relative changes of $PM_{2.5}$ chloride show drastic declines with NH_3 emissions reductions, but with the emissions used here the absolute contribution of chloride is small. The absolute change of $PM_{2.5}$ fine nitrate ranges from 0.0 to 4.3 μg/m^3 with NH_3 emissions removal, slightly less than that of $PM_{2.5}$ ammonium (1.0 – 5.0 μg/m^3). However, the relative changes of fine nitrate show more substantial declines than those of ammonium, decreasing by up to 100 % across the South Asia domain. The decline of nitrate accelerates from NH_3-rich to NH_3-poor environments, which highlights that NH_3 plays a critical role in nitrate formation, particularly under low NH_3 conditions, where ammonium nitrate formation is NH_3 limited. Similar phenomena are reported by previous studies (Xu et al., 2016; Han et al., 2020; Liu et al., 2021) that focused on China and globally (Gu et al., 2023). Additionally, nitrate virtually disappears already for 90 % NH_3 emissions reductions in some countries like Nepal, Bhutan, Sri Lanka and Afghanistan. In contrast to nitrate and ammonium, sulfate concentrations were predicted to increase as NH_3 emissions declined, with the largest relative increases in Nepal and Bhutan. These increases in sulfate can be attributed to co-deposition effects in the EMEP model, where the non-stomatal canopy uptake resistance of SO_2 increases with the mean molar SO_2/NH_3 ratio (Simpson et al., 2012), more sulfate formation is caused by a decline in dry deposition of SO_2 when less NH_3 is available to neutralize the SO_2 deposited to plant surfaces.

3.3. Health impacts and economic losses attributable to ambient $PM_{2.5}$ exposure due to NH_3 emissions

Exposure to ambient $PM_{2.5}$ concentrations can lead to adverse health impacts and economic losses. Here we estimate premature mortality and economic losses with the current emission data and explore the contribution of NH_3 emissions to these outcomes. Fig. S9 shows the population exposure to annual $PM_{2.5}$ concentration for the BASE run in South Asia. Approximately 1.8 billion people (95 % of the total population) are estimated to be exposed to annual $PM_{2.5}$ concentrations of between 20 and 90 μg/m^3 with all emission sectors included. Only around 2 million people (0.1 %) are predicted to experience levels $\leq$ 10 μg/m^3, meeting the WHO 4th interim target, and less than 10 thousand do not exceed the WHO annual air quality guideline of 5 μg/m^3. Annual mean $PM_{2.5}$ concentration varying with population density across South Asia is also shown in Fig. S9 (right). A clear increase in $PM_{2.5}$ concentrations can be observed with population density up to 3000 person/km^2. In other words, $PM_{2.5}$ concentrations follow human activity and are lower in areas with less population density and higher in regions where the population is large.

Per capita mortality and corresponding premature deaths due to annual mean $PM_{2.5}$ exposure in different locations across South Asia are illustrated in Fig. 7A, with specific values presented in Table 3. The estimated range of per capita mortality is 0.04–0.15 % with the

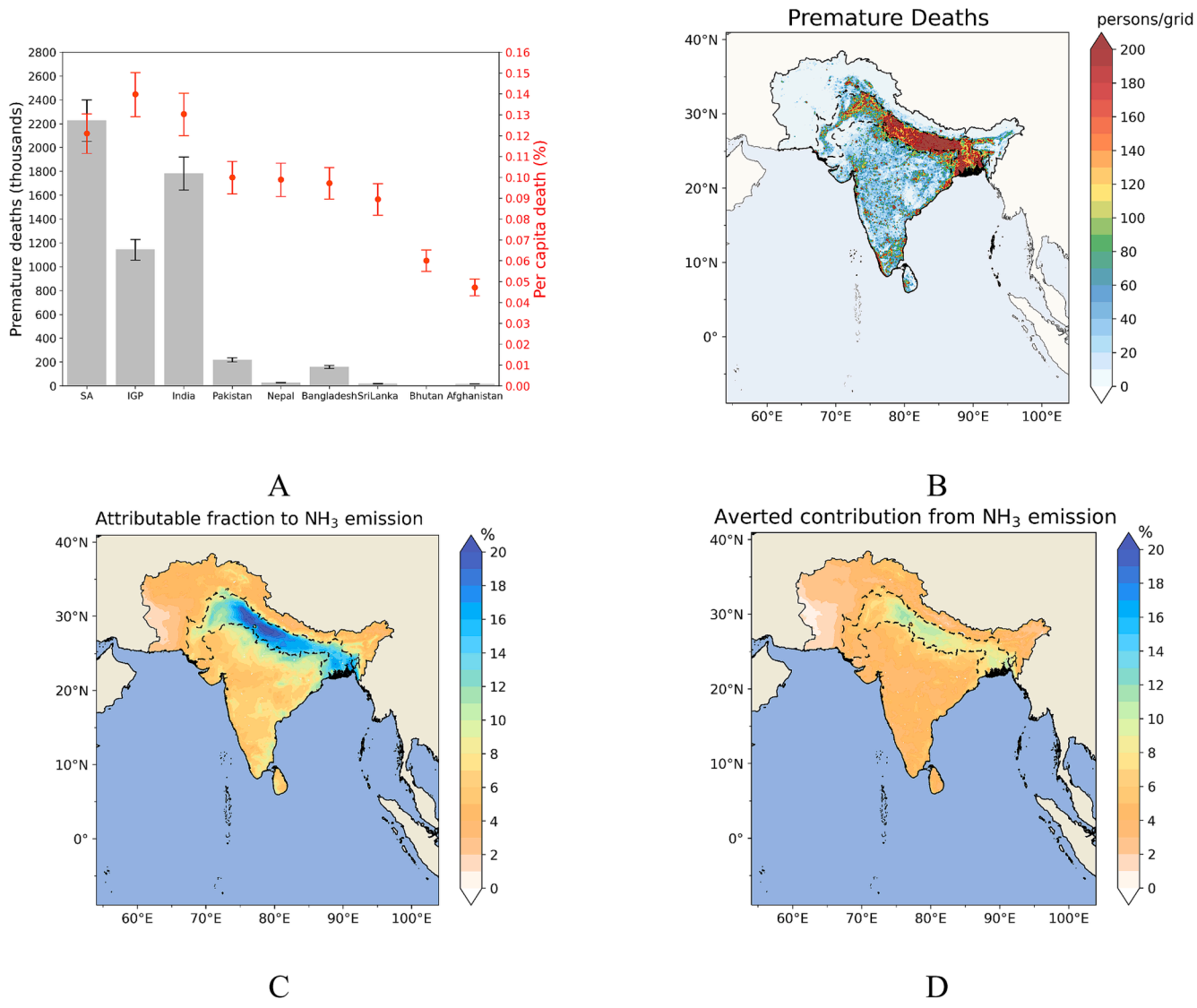

Fig. 7. Health impacts attributable to annual mean $PM_{2.5}$ exposure. A: premature deaths in different countries and regions with per capita death rates; B: spatial distribution of premature deaths in South Asia; C: spatial distribution of the attributable fraction of premature deaths from all NH_3 emissions (attribution method); D: spatial distribution of the averted contribution to premature deaths from removing all NH_3 emissions (subtraction methods).

maximum in the IGP and the minimum in Afghanistan. High per capita mortality is due to high baseline mortality rates and population-weighted $PM_{2.5}$ concentrations. The overall per capita mortality and premature deaths for South Asia are 0.12 % (95 % Confidence Interval: 0.11 %-0.13 %) and 2,228,000 (2,052,000–2,400,000) for the BASE run, respectively. Among all South Asian countries, India is estimated to experience the largest number of premature deaths due to $PM_{2.5}$ exposure (1,784,000; 1,643,000–1,921,000), followed by Pakistan (220,000; 202,000–236,000), together accounting for 90 % of total premature deaths due to annual mean $PM_{2.5}$ exposure in South Asia. These figures are significantly exceed estimated in the GBD study due to a newly updated concentration–response function used. Consistent with the spatial distribution of annual $PM_{2.5}$ and population, the greatest number of premature deaths identifies in the IGP (Fig. 7B), with approximately 1143,000 (1,055,000–1,228,000) mortalities attributable to ambient $PM_{2.5}$ exposure. We apply both the attribution method and subtraction method to assess health burdens from NH_3 emissions in this study. Fig. 7C presents the spatial distribution of the relative contribution of NH_3 emissions to $PM_{2.5}$ premature mortality, with values ranging from 1 to 45 %. The largest contributions occur in the IGP, some central and eastern coastal Indian cities and northern Pakistan. Estimated premature deaths due to $PM_{2.5}$ exposure from all NH_3 emissions across South Asia are 247,000 (227,000–265,000), calculated with the attribution method, accounting for 11 % of the total premature mortality from all emission sectors. In contrast, the contribution that NH_3 control could help avert, calculated with the subtraction method, ranges from 1 to 15 % (Fig. 7D) relating to 140,000 (132,000–149,000) premature deaths attributable to ambient $PM_{2.5}$ from all NH_3 emissions, accounting for 6 % of the total premature mortality from all sectors. The values derived from the subtraction approach are significantly smaller, by a factor of up to 2 than those obtained from the attribution approach. The discrepancy is primarily attributed to the strong nonlinearities in the GEMM exposure–response function.

Applying unit economic costs of mortality and VSL, we estimate the economic losses for South Asia in 2018. The total GDP of South Asia for that year was US$ 11.27 trillion (in 2017 at purchasing power parity (PPP), according to the World Bank (https://data.worldbank.org/)), and the total economic losses for this region are assessed at approximately US$ 596,000 (549,000–642,000) million for the base run, accounting for 5 % (5 %–6 %) of total annual GDP of South Asia (in 2017 US$ at PPP). Further details on the economic losses across various regions and countries are listed in Table 4. The attribution method estimates US$

Table 3
Estimated premature deaths (thousands) attributable to $PM_{2.5}$ due to all sectors and NH_3 emissions in 2018 across South Asia (SA) and the Indo-Gangetic Plain (IGP).

	Premature deaths (thousands)		
	All sectors	NH_3 emissions (Attribution method)	NH_3 emissions (Subtraction method)
SA	2228 (2052–2400)	247 (227–265)	140 (132–149)
IGP	1143 (1055–1228)	162 (149–174)	88 (83–93)
India	1784 (1643–1921)	198 (182–212)	111 (104–118)
Pakistan	220 (202–236)	21 (20–23)	12 (11–13)
Nepal	28 (26–30)	2 (2–3)	1 (1–2)
Bangladesh	159 (147–171)	23 (21–25)	14 (13–15)
Sri Lanka	19 (18–21)	1.5 (1.4–1.7)	1.0 (0.9–1.0)
Bhutan	0.5 (0.4–0.5)	0.02 (0.02–0.03)	0.01 (0.01–0.02)
Afghanistan	17 (16–19)	0.8 (0.7–0.9)	0.5 (0.4–0.6)

Table 4
Estimated economic losses (US$ million) attributable to $PM_{2.5}$ due to all sectors and NH_3 emissions in 2018.

	Economic losses (US$ million)		
	All sectors	NH_3 emissions (Attribution method)	NH_3 emissions (Subtraction method)
SA	596,000 (549,000–642,000)	66,000 (61,000–71,000)	37,000 (35,000–40,000)
IGP	301,000 (278,000–323,000)	43,000 (40,000–46,000)	23,000 (22,000–25,000)
India	491,000 (452,000–528,000)	54,000 (50,000–58,000)	31,000 (29,000–32,000)
Pakistan	54,000 (50,000–57,000)	5,300 (5,000–5,700)	3,000 (2,800–3,200)
Nepal	3,600 (3,300–4,000)	300 (280–330)	190 (170–200)
Bangladesh	33,000 (30,000–35,000)	4,700 (4,000–5,000)	2,800 (2600–3,000)
Sri Lanka	13,000 (12,00–14,000)	1,000 (900–1,100)	600 (580–680)
Bhutan	190 (171–200)	11 (10–12)	7 (6–8)
Afghanistan	1,800 (1,700–2,000)	84 (77–92)	54 (50–58)

66,000 (61,000–71,000) million economic losses due to NH_3 emissions alone, representing 11 % of the total economic losses in South Asia, while the economic losses calculated from the subtraction method are US$ 37,000 (35,000–40,000) million, which accounts for 6 % of the overall economic losses from all sectors across South Asia.

Fig. 8 illustrates how different levels of NH_3 emissions contribute to premature deaths and economic losses across South Asia in 2018. The attribution analysis estimates sector-specific mortality, assuming that the response of premature deaths and economic losses are similar to those observed for total $PM_{2.5}$ concentration. The subtraction approach assesses the level of reduction in premature mortality and economic losses could be achieved if a specific sector is removed. Results from the attribution method are by a factor of up to 2 larger than those are from the subtraction method. Changes in premature mortality and economic losses all follow non-linear variations with the level of emissions control, with values increasing at an accelerated pace when NH_3 emissions is reduced by 70 % or more. This finding emphasizes that a reduction of at least 70 % in NH_3 emission in South Asia could lead to significantly greater health and economic benefits. Furthermore, by fixing the ratios between the left and the right-hand-side scales in Fig. 8, it becomes obvious that in countries such as Sri Lanka and Bhutan, the gaps between premature deaths and economic losses are smaller compared to other countries. This is attributable to the higher economic costs of mortality in Sri Lanka and Bhutan than those in other South Asian countries (see Table 1).

3.4. Interactions with emission changes of SO_2 and NO_x

Some mitigation policies have been implemented in South Asian countries to address the high $PM_{2.5}$ concentrations. Among these abatement strategies, the primary focus has been on reducing SO_2 and NO_x emissions which are predominantly from residential, industrial, transport and power sectors. The reductions in SO_2 and NO_x emissions have a significant impact on the formation of SIA. Here we conduct two additional sensitivity tests to quantify the impact of NH_3 emissions reductions on $PM_{2.5}$ pollution alongside reductions in SO_2 and NO_x emissions. The first sensitivity test involves a simultaneous reduction of 30 % in both NH_3 and SO_2 emissions (defined as $S30_{NS}$), while the second test aims for a further 30 % reduction in NO_x emission on the top of the reductions in the first test (defined as $S30_{NSN}$). We chose a 30 % reduction because reducing 30 % NH_3 may be an achievable mitigation target (Sutton et al., 2011; Bittman et al., 2014).

Table 5 illustrates changes in $PM_{2.5}$ and its components between the BASE run and sensitivity tests in South Asian countries and the IGP. We estimated that 30 % reductions in SO_2, NO_x and NH_3 emissions represent about 17,000 Gg S, 10,700 Gg N and 13,000 Gg N annually over the South Asia domain, respectively. Throughout the South Asian countries, minor declines happen in SIA and $PM_{2.5}$ concentration with 30 % reduction in NH_3 emission alone, by contrast, a simultaneous 30 % reduction in NH_3 and SO_2 emissions leads to 26.2 % and 7.1 % decreases in SIA and $PM_{2.5}$ concentrations, respectively, highlighting their critical role in the formation of SIA. Furthermore, an additional 30 % reduction in NO_x emission results in substantial declines for all SIA components, with SIA and $PM_{2.5}$ concentrations dropping by 8.7 % and 29.8 %. Specifically, fine nitrate levels have the most significant reduction while Cl^- levels show a slight rise compared to the $S30_{NS}$ run. Additionally, according to the attribution method, 30 % reductions in SO_2, NO_x and NH_3 emissions collectively contributes to a reduction of 235,000 (216,000–253,000) premature deaths and US$ 63,000 (58,000–68,000) million in economic losses over South Asian countries (attribution method). These reductions are comparable to those achieved by a theoretical 100 % reduction in NH_3 emission alone. The changes in all air pollutants and $PM_{2.5}$-related impacts in the IGP slightly differ from those in all countries. These findings emphasize the necessity for joint emission controls targeting SO_2, NO_x, and NH_3 for comprehensive mitigation of ambient $PM_{2.5}$ pollution in South Asia.

4. Discussion

In the current study, the atmospheric chemical transport modelling system WRF-EMEP with a new estimate of anthropogenic NH_3 emissions is applied at 0.11° resolution to assess the impacts of NH_3 emissions control strategies on $PM_{2.5}$ pollution, as well as the related premature human deaths and economic losses over South Asia in 2018 associated with long-term exposure. Results show that model simulations can reproduce magnitudes and variations of $PM_{2.5}$. Total ambient $PM_{2.5}$ attribute 2,228,000 (95 % CI: 2,052,000–2,400,000) premature deaths and US$ 596,000 (95 % CI: 549,000–642,000) million economic losses·NH_3 emissions contribute 11 % to the annual $PM_{2.5}$ levels, with significant health and economic losses (247,000 premature deaths (95 % CI: 227,000–265,000) and US$ 66,000 (95 %CI: 61,000–71,000) million).

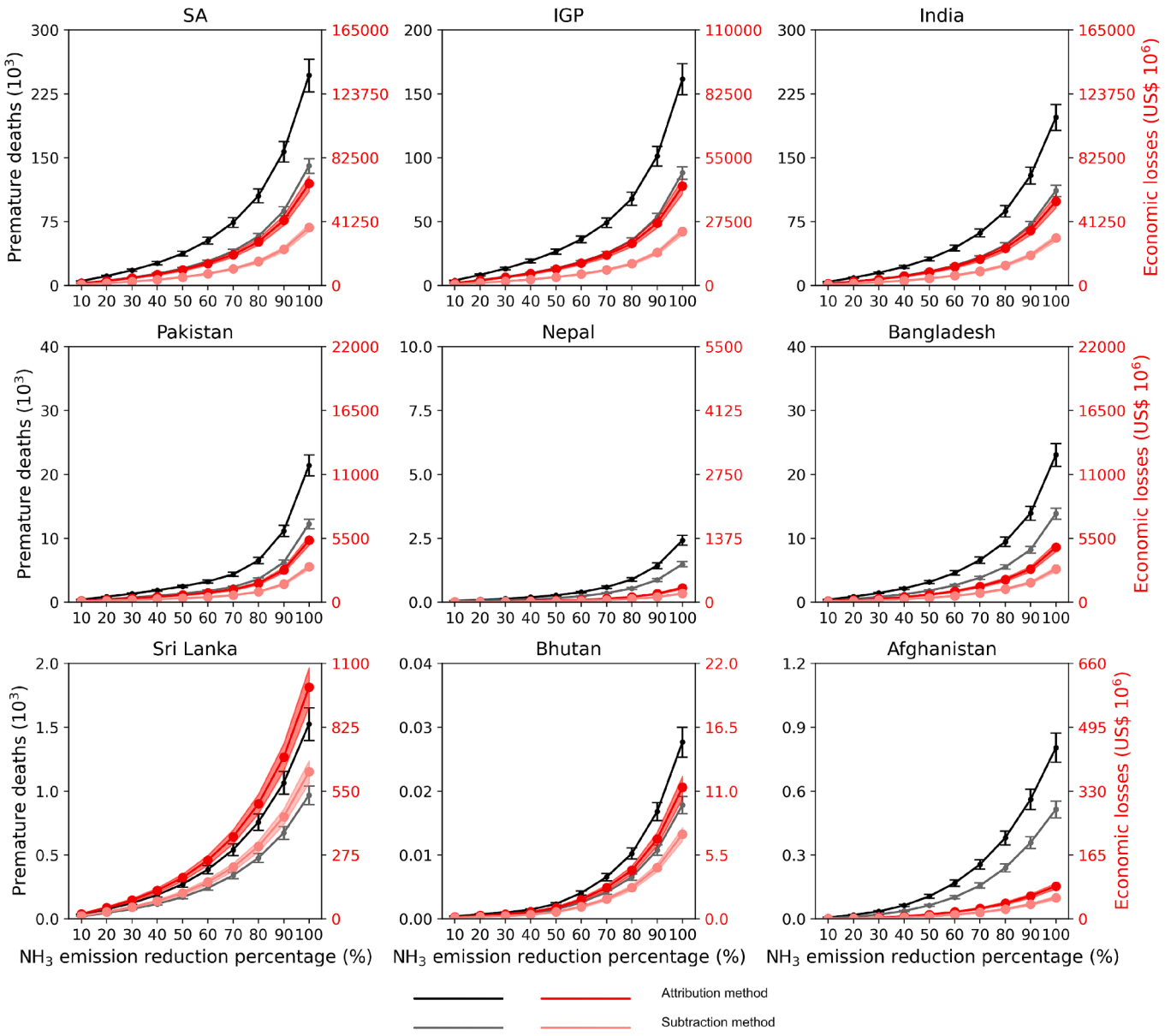

Fig. 8. Premature deaths and economic losses attributable to NH_3 emissions in 2018. The dark lines represent results from the attribution method, and the light lines represent results from the subtraction method.

Table 5
The annual relative change (%) of $PM_{2.5}$, its component concentrations and its impacts based on attribution method between the BASE and sensitivity tests in South Asian countries and IGP.

		NH_3 emissions reduction	SO_4^{2-}	NO_3^-	NH_4^+	Cl^-	SIA	$PM_{2.5}$	Premature deaths	Economic losses
SA	$S30_N$-BASE	30 % NH_3	2.2	−18.1	−5.0	−30.0	−2.4	−0.6	−0.8	−0.8
	$S30_{NS}$-BASE	30 %NH_3 + 30 %SO_2	−27.0	−14.6	−26.8	−23.4	−26.2	−7.1	−7.3	−7.3
	$S30_{NSN}$-BASE	30 % NH_3	−28.8	−41.5	−30.0	−18.6	−29.8	−8.7	−10.5	−10.5
IGP	$S30_N$-BASE	30 % NH_3	2.2	−14.5	−3.8	−27.3	−3.8	−1.1	−1.2	−1.2
	$S30_{NS}$-BASE	30 %NH_3 + 30 %SO_2	−28.0	−11.2	−23.0	−25.6	−22.3	−6.8	−6.8	−6.8
	$S30_{NSN}$-BASE	30 %NH_3 + 30 %SO_2 + 30 %NO_x	−30.4	−37.4	−32.4	−21.6	−32.8	−10.8	−10.9	−10.9

4.1. Comparisons with other studies

A comparison of studies of premature deaths due to ambient $PM_{2.5}$ exposure across South Asian countries is shown in Table S3. Our estimates of 2,228,000 (2,052,000–2,400,000) from all sectors across South Asia in 2018, and 1,784,000 (1,643,000–1,921,000) in India are consistent with previous studies (Cohen et al., 2017; Pozzer et al., 2017; Conibear et al., 2018; Pandey et al., 2021; Maji et al., 2023). Premature deaths based on GEMM exposure–response function are higher than those derived using the IER model. The GEMM incorporates data from a Chinese cohort study covering a wide range of $PM_{2.5}$ concentrations, which helps to reduce these uncertainties (Burnett et al., 2018; Lelieveld

et al., 2020). Moreover, the GEMM function in this study considers all non-communicable diseases plus lower respiratory infections (NCD + LRI), while the IER model is limited to only five specific diseases, including stroke, ischemic heart disease, chronic obstructive pulmonary disease, lung cancer and lower respiratory infections. In addition to applying different exposure–response functions, the discrepancies among these studies largely attributed to differences in annual $PM_{2.5}$ concentrations, stemming from different approaches, emissions, and resolutions. The study by Maji et al. (2023) reported higher premature mortality based on the finer resolution of ground level $PM_{2.5}$ data. However, the $PM_{2.5}$ concentrations used in their analysis are derived from aerosol optical depth retrievals applying statistical methods and downscaled meteorological variables (van Donkelaar et al., 2021), suggesting the reliable data content is not as high as what the resolution implies (Wang et al., 2020).

Using a coarse resolution global model and the subtraction method, Lelieveld et al. (2015) evaluated premature deaths due to $PM_{2.5}$ resulting from agricultural emissions in India, Pakistan, Bangladesh, and Nepal at 40,000; 1,900; 9,000 and 400, respectively. These estimates are lower compared with our findings using the subtraction method (Table 3). The main reasons for these discrepancies likely include the temporal and spatial variations in agricultural emissions, differences in model resolution, mechanisms and concentration–response functions.

The economic losses in our study amount to 596,000 (549,000–642,000) million US$, 11 % of these due to NH_3 emissions based on the attribution method. In contrast, only 6 % can be addressed through NH_3 emissions reductions, based on the subtraction method. The World Bank (2016) reported economic losses of 253,000 million US $ due to ambient $PM_{2.5}$ pollution in 2013 over South Asia, with India accounting for 81 % of these losses (Table S4). Our results are consistent with the World Bank's findings, air pollution, particularly the ambient $PM_{2.5}$ pollution, has emerged as one of the most severe environmental issues in South Asia over the last decade, which results in large and increasing economic losses.

4.2. Uncertainties

Although NH_3 emissions are here perturbed at the global scale, the South Asia region is sufficiently large that most of the benefit in concentration decreases are due to emission reduction within the region itself.

Persistently high chloride concentrations have been reported in Delhi and other Indian cities (Gunthe et al 2021; Chen et al., 2022), suggesting an excess of available NH_3 neutralized hydrochloric acid to form ammonium chloride, subsequently increasing $PM_{2.5}$ concentrations. In our study chloride predicted chloride concentrations are significantly lower than those observed in Delhi, which indicates substantial uncertainties in local emissions of hydrochloric acid and NH_3 in South Asia, particularly in densely populated urban areas. Hence, our findings possibly underestimate the contribution from NH_3 to $PM_{2.5}$ formation and its related health impacts, as well as the $PM_{2.5}$ response to NH_3 emissions changes. To address these uncertainties, future work will incorporate direct speciated aerosol measurements to refine our understanding of HCl emissions and thus the impacts of NH_3 on $PM_{2.5}$ concentrations. For example, focusing on Delhi, Pawar et al. (2023) obtained an improved model fit to the measurements for a winter month by adjusting emissions of HCl and NH_3.

In the precious and current studies, the long-term health burdens were evaluated using exposure–response functions between the total mass concentrations of $PM_{2.5}$ and the health endpoints, assuming equal toxicity for different chemical components of $PM_{2.5}$. $PM_{2.5}$ is the aerosol metric for which most epidemiological evidence of dose–response functions has been derived. This is driven by the large amount of data available for $PM_{2.5}$. However, several studies have suggested that the toxicities of chemical compositions from various sources affect the health impacts of $PM_{2.5}$ differently (Franklin et al., 2008; Atkinson et al., 2015; Ostro et al., 2015). Estimates of health burdens due to ambient $PM_{2.5}$ would be more precise if the effect modifications of individual chemical components were incorporated into risk assessments (Li et al., 2021). In addition, $PM_{2.5}$ contains constituents a range of particularly hazardous air pollution (e.g. PAHs, some heavy metals) for which concentration thresholds for some hazardous air pollutants have been provided e.g. by the US EPA, and some studies used the Incremental Lifetime Cancer Risk model to express the probability of developing cancer over a lifetime due to exposure particle borne carcinogens (Watanabe et al., 2010; U.S.EPA 2011a, 2011b). However, the concentrations of these compounds are not affected by ammonia emission control and these additional health assessments are therefore not included here.

Apart from different chemical compositions, the health impact of $PM_{2.5}$ is likely influenced by aerosol size distribution (Kumar et al., 2014; Ostro et al., 2015). Fine and ultrafine particles, which are inhalable and can penetrate the respiratory system more deeply and possibly cross cell membranes, lead to greater health effects (Mitsakou et al., 2007; Zwozdziak et al., 2017). These findings suggest that to improve the assessment of long-term health impacts and optimize emission reduction policies, researchers should develop and update exposure–response functions or coefficients, considering chemical compositions, size distribution and sources of ambient $PM_{2.5}$. This would require a step change in measurement stations targeting these additional metrics. For the time being the international consensus is that information on differential toxicity is too limited to consider chemical composition in health impact assessments (COMEAP, 2022; U.S. EPA, 2019; WHO 2021).

Additionally, whilst our study focused on estimating health impacts due to long-term $PM_{2.5}$ exposure, the short-term acute exposure to high $PM_{2.5}$ on daily timescales can also be important (Pop III, 2000). Here we used a Poisson regression function to estimate the acute total non-accidental number of mortalities due to high $PM_{2.5}$ concentrations during pollution episodes over annual timescales across South Asia, this approach has been applied widely in the epidemiology of air pollution (Wang and Mauzerall, 2006; Gao et al., 2015). Due to a lack of studies providing the hazard ratios (the magnitude of the association between $PM_{2.5}$ exposure and the probability of death) for South Asian countries, we applied hazard ratios from a *meta*-analysis of the coefficients associating short-term $PM_{2.5}$ exposure and health responses in China (Lu et al., 2015). We find a total of 121,000 (95 % CI: 67,000–177,000) acute mortalities over South Asia, estimated acute deaths due to daily $PM_{2.5}$ exposure from NH_3 emissions across South Asia are 15,000 (9,000–22,000) based on the attribution method, accounting for 13 % of total acute deaths from all emission sectors. This equates to 5.4 % of the health impacts from long-term exposure for all sources, and 6 % for the ammonia impact, indicating that long-term exposure is the dominant mechanism, but that SIA production from ammonia makes a somewhat larger contribution to peak daily concentrations (used for the assessment of short-term exposure) than for annual average concentrations. More details about the related method and results are provided in the Supplementary (Section S1 and Table S5).

Mitigating NH_3 emission will lead to significant reductions in $PM_{2.5}$ as well as improve health benefits, however, as a major alkaline gas in the atmosphere, NH_3 emissions reductions will affect acids in the aerosol and cloud liquid phase neutralization, thus increasing the acidity of aerosol particles (Behera et al., 2013). Aerosol pH is crucial in the reactive uptake of gases, which can influence ozone chemistry and various particle characteristics, including the scattering efficiency, deposition processes and hygroscopic growth (Karydis V.A et al., 2021). Pozzer et al. (2017) highlighted that $PM_{2.5}$ pH was found to be particularly sensitive to reductions in NH_3 emissions over South Asia, with aerosol pH decreasing by 1.72 pH units upon the removal of all NH_3 emissions. High acidic aerosols enhance the solubility of trace metals associated with toxicity (Oakes et al., 2012; Fang et al., 2017) from anthropogenic and mineral sources, which have detrimental health

impacts on human respiratory by generating reactive oxygen species (Raizenne et al., 1996; Weber et al., 2016). Therefore, the potential increase in aerosol acidity could counteract the air quality benefits achieved by controlling NH_3 emissions, and the current concentration–response functions are not reflected the variability in aerosol acidity.

Fig. S10a shows that at the annual average over the entire South Asian region hydrogen ion (H^+) concentration increases as NH_3 emissions decrease in our calculations. However, the prevalence of H + is spatially variable. At baseline emissions most of South Asia is characterized by large concentrations of free NH_3 and the aerosol is therefore fully neutralized, even at the annual average (Fig. S10b), and in these areas substantial emission reduction is required to significantly affect aerosol acidity. Acidic aerosol already exists in the less intensely agricultural areas in Afghanistan and Pakistan, near industrial SO_2 sources around Kolkata, India, and above the sea, and it is these regions that drive the South Asian H^+ response at the lower NH_3 emission reductions (Fig. S10c).

It should be noticed that this analysis does not fully consider the chemical impact of alkaline soil dust. Soil dust from certain regions of South Asia, e.g. Afghanistan, southern Pakistan, and the Indian subcontinent during dry season, can contribute significantly to $PM_{2.5}$ (Kulshrestha et al., 2001; Karydis et al., 2016). Further study is needed to fully understand the net impact on $PM_{2.5}$ acidity in South Asia.

The formation of ammonium aerosols depends on thermodynamic equilibrium influenced by temperature, relative humidity and chemical compositions (Pio and Harrison, 1987). High relative humidity and low temperatures favor their formation, while warmer conditions cause them to volatilize (Ianniello et al., 2011). The thermodynamic scheme EQSAM4clim was used in the EMEP model to represent these processes (Simpson et al., 2012). High temperature can also potentially enhance NH_3 emissions (Mark et al., 2013), however, it is challenging to estimate ammonia emissions in relation to meteorology, as it requires integrating all activity data into the atmospheric chemical transport models, which has only been accomplished in limited countries and studies.

The WRF-EMEP model provides an estimate of $PM_{2.5}$ pollution in South Asia and it is used to investigate sector-specific contributions. Compared to regions like North America, Europe and East Asia, South Asia has fewer measurement sites, observed species and data are often collected at a lower spatial resolution. Enhancing the accessibility of valid measurements would be beneficial to reduce the uncertainties that associated with atmospheric chemistry modelling. This said, the performance of the WRF-EMEP model has been thoroughly assessed across the world in many previous studies (Dong et al., 2018; Jonson et al., 2022; Whaley et al., 2023), which makes our findings reliable and robust.

5. Conclusions

The emission levels of NH_3 in South Asia are substantial and have a significant impact on regional air pollution. As a precursor of secondary aerosols, accurately capturing the nonlinear process of these aerosols' formation is essential to understand the role of NH_3 in $PM_{2.5}$ pollution. Sensitivity tests demonstrate that all $PM_{2.5}$ concentrations decrease rapidly when NH_3 emissions reductions exceed 70 %. Particulate nitrate (NO_3^-) shows a more substantial decline than ammonium, and the decline accelerates from NH_3-rich to a NH_3-poor environments, indicating a significant contribution of NH_3 to nitrate formation under low-NH_3 conditions. It is also important to estimate human health impacts and economic losses attributable to ambient $PM_{2.5}$ associated with NH_3 emissions reductions. We use attribution method and subtraction method to estimate premature mortality associated with NH_3 emissions, the former estimates NH_3 emissions accounts for 11 % of the total premature mortality from all sectors, which are by a factor of up 2 larger than those derived from the subtraction approach over the South Asian countries. This discrepancy is primarily attributed to the strong nonlinearities in the GEMM exposure–response function.

This study indicates that the impacts of NH_3 on $PM_{2.5}$ pollution are complex, largely attributed to the nonlinear features of secondary inorganic aerosols formation. The effectiveness of $PM_{2.5}$ reduction shows only moderate sensitivity to the intensity of NH_3 emissions reductions alone. Thus, it is important to implement joint controls on SO_2, NO_x and NH_3 emissions controls to achieve significant mitigation of ambient $PM_{2.5}$ and improve air quality in South Asia.

CRediT authorship contribution statement

Yuanlin Wang: Writing – original draft, Visualization, Validation, Formal analysis, Conceptualization. **Eiko Nemitz:** Writing – review & editing, Methodology, Formal analysis, Conceptualization. **Samuel J. Tomlinson:** Writing – review & editing, Validation, Methodology, Formal analysis. **Edward J. Carnell:** Data curation. **Liquan Yao:** Writing – review & editing, Conceptualization. **Janice Scheffler:** Methodology. **Tomas Liska:** Validation. **Clare Pearson:** Data curation. **Ulrike Dragosits:** Writing – review & editing, Resources. **Chandra Venkataraman:** Writing – review & editing, Methodology. **Srinidhi Balasubramanian:** Writing – review & editing. **Rachel Beck:** Validation. **Mark A. Sutton:** . **Massimo Vieno:** Writing – review & editing, Validation, Resources, Methodology.

Declaration of competing interest

The authors declare that they have no known competing financial interests or personal relationships that could have appeared to influence the work reported in this paper.

Acknowledgements

This work was carried out within the South Asian Nitrogen Hub funded by the UK Global Challenges Research Fund (GCRF) of UKRI administered by the Natural Environment Research Council (NERC) (NE/S009019/1). It was further supported by NERC as part of the NC for Global Challenges: International Science for Net Zero Plus Programme (NE/X006247/1), as well as supported by NERC as part of UK-SCAPE Programme (NE/R016429/1) and ACCESS-UK Programme (NE/Y006208/1), all contributing to the delivery of National Capability.

Appendix A. Supplementary data

Supplementary data to this article can be found online at https://doi.org/10.1016/j.envint.2024.109207.

Data availability

Data will be made available on request.

References

Agarwal, P., Stevenson, D.S., Heal, M.R., 2023. Evaluation of WRF-Chem simulated meteorology and aerosols over northern India during the severe pollution episode of 2016. Egusphere 2023, 1–43. https://doi.org/10.5194/acp-24-2239-2024.

Atkinson, R.W., Mills, I.C., Walton, H.A., Anderson, H.R., 2015. Fine particle components and health—a systematic review and meta-analysis of epidemiological time series studies of daily mortality and hospital admissions. J. Eposure Sci. Environ. Epidemiol. 25 (2), 208–214. https://doi.org/10.1038/jes.2014.63.

Balasubramanian, S., McFarland, D.M., Koloutsou-Vakakis, S., Fu, K., Menon, R., Lehmann, C., Rood, M.J., 2020. Effect of grid resolution and spatial representation of NH3 emissions from fertilizer application on predictions of NH3 and PM2. 5 concentrations in the United States Corn Belt. Environ. Res. Commun. 2 (2), 025001. https://doi.org/10.1088/2515-7620/ab6c01.

Behera, S.N., Sharma, M., Aneja, V.P., Balasubramanian, R., 2013. Ammonia in the atmosphere: a review on emission sources, atmospheric chemistry and deposition on terrestrial bodies. Environ. Sci. Pollut. Res. 20, 8092–8131. https://doi.org/10.1007/s11356-013-2051-9.

Berge, E., Jakobsen, H.A., 1998. A regional scale multilayer model for the calculation of long-term transport and deposition of air pollution in Europe. Tellus B 50 (3), 205–223. https://doi.org/10.1034/j.1600-0889.1998.t01-2-00001.x.

Bittman, S., Dedina, M.C.M.H., Howard, C.M., Oenema, O. and Sutton, M.A., (eds) 2014. Options for ammonia mitigation: Guidance from the UNECE Task Force on Reactive Nitrogen. NERC/Centre for Ecology & Hydrology.

Boylan, J.W., Russell, A.G., 2006. PM and light extinction model performance metrics, goals, and criteria for three-dimensional air quality models. Atmos. Environ. 40 (26), 4946–4959. https://doi.org/10.1016/j.atmosenv.2005.09.087.

Burnett, R., Chen, H., Szyszkowicz, M., Fann, N., Hubbell, B., Pope III, C.A., Apte, J.S., Brauer, M., Cohen, A., Weichenthal, S., Coggins, J., 2018. Global estimates of mortality associated with long-term exposure to outdoor fine particulate matter. Proc. Natl. Acad. Sci. 115 (38), 9592–9597. https://doi.org/10.1021/acs.est.0c01764.s001.

Burnett, R.T., Pope III, C.A., Ezzati, M., Olives, C., Lim, S.S., Mehta, S., Shin, H.H., Singh, G., Hubbell, B., Brauer, M., Anderson, H.R., 2014. An integrated risk function for estimating the global burden of disease attributable to ambient fine particulate matter exposure. Environ. Health Perspect. 122 (4), 397–403. https://doi.org/10.1289/ehp.122-a235.

Cash, J.M., Langford, B., Di Marco, C., Mullinger, N., Allan, J., Reyes-Villegas, E., Joshi, R., Heal, M.R., Acton, W.J.F., Hewitt, N., Misztal, P., 2020. Seasonal analysis of submicron aerosol in Old Delhi using high resolution aerosol mass spectrometry: Chemical characterisation, source apportionment and new marker identification. Atmospheric Chemistry and Physics Discussions 2020, 1–42. https://doi.org/10.5194/acp-21-10133-2021.

Chang, J.S., 1989. The role of H2O and NH3 on the formation of NH4NO3 aerosol particles and De-NOx under the corona discharge treatment of combustion flue gases. J. Aerosol Sci 20 (8), 1087–1090. https://doi.org/10.1016/0021-8502(89)90768-4.

Chatterjee, D., McDuffie, E.E., Smith, S.J., Bindle, L., van Donkelaar, A., Hammer, M.S., Venkataraman, C., Brauer, M., Martin, R.V., 2023. Source Contributions to Fine Particulate Matter and Attributable Mortality in India and the Surrounding Region. Environ. Sci. Tech. 57 (28), 10263–10275. https://doi.org/10.1021/acs.est.2c07641.s001.

Chen, F. and Dudhia, J., 2001. Coupling an advanced land surface–hydrology model with the Penn State–NCAR MM5 modeling system. Part I: Model implementation and sensitivity. Monthly weather review, 129(4), 569-585. Doi: 10.1175/1520-0493(2001)129<0569:caalsh>2.0.co;2.

Chen, Y., Beig, G., Archer-Nicholls, S., Drysdale, W., Acton, W.J.F., Lowe, D., Nelson, B., Lee, J., Ran, L., Wang, Y., Wu, Z., 2021. Avoiding high ozone pollution in Delhi, India. Faraday Discuss. 226, 502–514. https://doi.org/10.1039/d0fd00079e.

Chen, Y., Wang, Y., Nenes, A., Wild, O., Song, S., Hu, D., Liu, D., He, J., Hildebrandt Ruiz, L., Apte, J.S., Gunthe, S.S., 2022. Ammonium chloride associated aerosol liquid water enhances haze in Delhi. India. Environmental Science & Technology 56 (11), 7163–7173. https://doi.org/10.1021/acs.est.2c00650.

Chowdhury, S., Dey, S., 2016. Cause-specific premature death from ambient PM2. 5 exposure in India: Estimate adjusted for baseline mortality. Environ. Int. 91, 283–290. https://doi.org/10.1016/j.envint.2016.03.004.

Cohen, A.J., Brauer, M., Burnett, R., Anderson, H.R., Frostad, J., Estep, K., Balakrishnan, K., Brunekreef, B., Dandona, L., Dandona, R., Feigin, V., 2017. Estimates and 25-year trends of the global burden of disease attributable to ambient air pollution: an analysis of data from the Global Burden of Diseases Study 2015. Lancet 389 (10082), 1907–1918. https://doi.org/10.1016/s0140-6736(17)30505-6.

COMEAP, 2022. Statement on the evidence for differential toxicity of particulate matter according to source or constituents: 2022. Available: https://www.gov.uk/government/publications/particulate-air-pollution-health-effects-of-exposure/statement-on-the-differential-toxicity-of-particulate-matter-according-to-source-or-constituents-2022.

Conibear, L., Butt, E.W., Knote, C., Arnold, S.R., Spracklen, D.V., 2018. Residential energy use emissions dominate health impacts from exposure to ambient particulate matter in India. Nat. Commun. 9 (1), 617. https://doi.org/10.1038/s41467-018-02986-7.

Cox, D.R., 1972. Regression models and life-tables. J. Roy. Stat. Soc.: Ser. B (Methodol.) 34 (2), 187–202. https://doi.org/10.1007/978-1-4612-4380-9_37.

Crippa, M., Guizzardi, D., Butler, T., Keating, T., Wu, R., Kaminski, J., Kuenen, J., Kurokawa, J., Chatani, S., Morikawa, T. and Pouliot, G., 2023. The HTAP_v3 emission mosaic: merging regional and global monthly emissions (2000–2018) to support air quality modelling and policies. Earth System Science Data (Online), 15 (PNNL-SA-182701). Doi: 10.5194/essd-15-2667-2023.

Crippa, M., Guizzardi, D., Muntean, M., Schaaf, E., Dentener, F., van Aardenne, J.A., Monni, S., Doering, U., Olivier, J.G.J., Pagliari, V., Janssens-Maenhout, G., 2018. Gridded emissions of air pollutants for the period 1970–2012 within EDGAR v4.3.2. Earth Syst. Sci. Data 10, 1987–2013. https://doi.org/10.5194/essd-10-1987-2018.

Donahue, N.M., Robinson, A.L., Pandis, S.N., 2009. Atmospheric organic particulate matter: From smoke to secondary organic aerosol. Atmospheric Environment 43 (1), 94–106. https://doi.org/10.1016/j.atmosenv.2008.09.055.

Dong, X., Fu, J.S., Zhu, Q., Sun, J., Tan, J., Keating, T., Sekiya, T., Sudo, K., Emmons, L., Tilmes, S., Jonson, J.E., 2018. Long-range transport impacts on surface aerosol concentrations and the contributions to haze events in China: an HTAP2 multi-model study. Atmos. Chem. Phys. 18 (21), 15581–15600. https://doi.org/10.5194/acp-18-15581-2018.

Dudhia, J., 1989. Numerical study of convection observed during the winter monsoon experiment using a mesoscale two-dimensional model. Journal of Atmospheric Sciences 46 (20), 3077–3107. https://doi.org/10.1175/1520-0469(1989)046<3077:nsocod>2.0.co;2.

Fang, T., Guo, H., Zeng, L., Verma, V., Nenes, A., Weber, R.J., 2017. Highly acidic ambient particles, soluble metals, and oxidative potential: a link between sulfate and aerosol toxicity. Environ. Sci. Tech. 51 (5), 2611–2620. https://doi.org/10.1021/acs.est.6b06151.

Franklin, M., Koutrakis, P., Schwartz, J., 2008. The role of particle composition on the association between PM2. 5 and mortality. Epidemiology 19 (5), 680–689. https://doi.org/10.1097/EDE.0b013e3181812bb7.

Gao, M., Guttikunda, S.K., Carmichael, G.R., Wang, Y., Liu, Z., Stanier, C.O., Saide, P.E., Yu, M., 2015. Health impacts and economic losses assessment of the 2013 severe haze event in Beijing area. Sci. Total Environ. 511, 553–561.

Gao, M., Beig, G., Song, S., Zhang, H., Hu, J., Ying, Q., Liang, F., Liu, Y., Wang, H., Lu, X., Zhu, T., 2018. The impact of power generation emissions on ambient PM2. 5 pollution and human health in China and India. Environ. Int. 121, 250–259. https://doi.org/10.1016/j.envint.2018.09.015.

Ge, Y., Heal, M.R., Stevenson, D.S., Wind, P. and Vieno, M., 2021. Evaluation of global EMEP MSC-W (rv4. 34) WRF (v3. 9.1. 1) model surface concentrations and wet deposition of reactive N and S with measurements. Geoscientific Model Development, 14(11), 7021-7046. Doi: 10.5194/gmd-14-7021-2021.

Ge, Y., Vieno, M., Stevenson, D.S., Wind, P., Heal, M.R., 2023. Global sensitivities of reactive N and S gas and particle concentrations and deposition to precursor emissions reductions. Atmos. Chem. Phys. 23 (11), 6083–6112. https://doi.org/10.5194/acp-23-6083-2023.

Gray, H.A., Cass, G.R., Huntzicker, J.J., Heyerdahl, E.K., Rau, J.A., 1986. Characteristics of atmospheric organic and elemental carbon particle concentrations in Los Angeles. Environ. Sci. Tech. 20 (6), 580–589. https://doi.org/10.1021/es00148a006.

Gu, B., Zhang, L., Van Dingenen, R., Vieno, M., Van Grinsven, H.J., Zhang, X., Zhang, S., Chen, Y., Wang, S., Ren, C., Rao, S., 2021. Abating ammonia is more cost-effective than nitrogen oxides for mitigating $PM_{2.5}$ air pollution. Science 374 (6568), 758–762. https://doi.org/10.1126/science.abf8623.

Gunthe, S.S., Liu, P., Panda, U., Raj, S.S., Sharma, A., Darbyshire, E., Reyes-Villegas, E., Allan, J., Chen, Y., Wang, X., Song, S., 2021. Enhanced aerosol particle growth sustained by high continental chlorine emission in India. Nat. Geosci. 14 (2), 77–84. https://doi.org/10.1038/s41561-020-00677-x.

Han, X., Zhu, L., Liu, M., Song, Y., Zhang, M., 2020. Numerical analysis of agricultural emissions impacts on $PM_{2.5}$ in China using a high-resolution ammonia emission inventory. Atmos. Chem. Phys. 20 (16), 9979–9996. https://doi.org/10.5194/acp-20-9979-2020.

Heitzenberg, J., 1989. Fine particles in the global troposphere A review. Tellus B 41 (2), 149–160. https://doi.org/10.1111/j.1600-0889.1989.tb00132.x.

Hewitt, C.N., 2001. The atmospheric chemistry of sulphur and nitrogen in power station plumes. Atmos. Environ. 35 (7), 1155–1170. https://doi.org/10.1016/S1352-2310(00)00463-5.

Hong, S.Y., Noh, Y., Dudhia, J., 2006. A new vertical diffusion package with an explicit treatment of entrainment processes. Monthly Weather Review 134 (9), 2318–2341. https://doi.org/10.1175/mwr3199.1.

Ianniello, A., Spataro, F., Esposito, G., Allegrini, I., Hu, M., Zhu, T., 2011. Chemical characteristics of inorganic ammonium salts in PM 2.5 in the atmosphere of Beijing (China). Atmos. Chem. Phys. 11 (21), 10803–10822. https://doi.org/10.5194/acp-11-10803-2011.

Islam, S.M.S., Uddin, R., Das, S., Ahmed, S.I., Zaman, S.B., Alif, S.M., Hossen, M.T., Sarker, M., Siopis, G., Livingstone, K.M., Mehlman, M.L., 2023. The burden of diseases and risk factors in Bangladesh, 1990–2019: a systematic analysis for the Global Burden of Disease Study 2019. Lancet Glob. Health 11 (12), e1931–e1942. https://doi.org/10.1016/S2214-109X(23)00432-1.

Janssens-Maenhout, G., Crippa, M., Guizzardi, D., Muntean, M., Schaaf, E., Dentener, F., Bergamaschi, P., Pagliari, V., Olivier, J.G., Peters, J.A., Van Aardenne, J.A., 2019. EDGAR v4. 3.2 Global Atlas of the three major greenhouse gas emissions for the period 1970–2012. Earth System Science Data 11 (3), 959–1002. https://doi.org/10.5194/essd-2017-79.

Jonson, J.E., Fagerli, H., Scheuschner, T., Tsyro, S., 2022. Modelling changes in secondary inorganic aerosol formation and nitrogen deposition in Europe from 2005 to 2030. Atmos. Chem. Phys. 22 (2), 1311–1331. https://doi.org/10.5194/acp-22-1311-2022.

Kain, J.S. and Fritsch, J.M., 1993. Convective parameterization for mesoscale models: The Kain-Fritsch scheme. In The representation of cumulus convection in numerical models (165-170). Boston, MA: American Meteorological Society. Doi: 10.1007/978-1-935704-13-3_16.

Karydis, V.A., Tsimpidi, A.P., Pozzer, A. and Lelieveld, J., 2021. How alkaline compounds control atmospheric aerosol particle acidity. Atmospheric chemistry and physics, 21(19).14983-15001. Doi: 10.5194/acp-21-14983-2021.

Karydis, V.A., Tsimpidi, A.P., Pozzer, A., Astitha, M., Lelieveld, J., 2016. Effects of mineral dust on global atmospheric nitrate concentrations. Atmos. Chem. Phys. 16 (3), 1491–1509. https://doi.org/10.5194/acp-16-1491-2016.

Kulshrestha, U.C., Kulshrestha, M.J., Sekar, R., Vairamani, M., Sarkar, A.K., Parashar, D. C., 2001. Investigation of alkaline nature of rain water in India. Water Air Soil Pollut. 130, 1685–1690. https://doi.org/10.1023/A:1013937906261.

Kumar, P., Morawska, L., Birmili, W., Paasonen, P., Hu, M., Kulmala, M., Harrison, R.M., Norford, L., Britter, R., 2014. Ultrafine particles in cities. Environ. Int. 66, 1–10. https://doi.org/10.1016/j.envint.2014.01.013.

Kurokawa, J., Ohara, T., Morikawa, T., Hanayama, S., Janssens-Maenhout, G., Fukui, T., Kawashima, K., Akimoto, H., 2013. Emissions of air pollutants and greenhouse gases over Asian regions during 2000–2008: Regional Emission inventory in Asia (REAS) version 2. Atmos. Chem. Phys. 13 (21), 11019–11058. https://doi.org/10.5194/acp-13-11019-2013.

Kuttippurath, J., Singh, A., Dash, S.P., Mallick, N., Clerbaux, C., Van Damme, M., Clarisse, L., Coheur, P.F., Raj, S., Abbhishek, K., Varikoden, H., 2020. Record high

levels of atmospheric ammonia over India: Spatial and temporal analyses. Sci. Total Environ. 740, 139986. https://doi.org/10.1016/j.scitotenv.2020.139986.
Lelieveld, J., Evans, J.S., Fnais, M., Giannadaki, D., Pozzer, A., 2015. The contribution of outdoor air pollution sources to premature mortality on a global scale. Nature 525 (7569), 367–371. https://doi.org/10.1038/nature15371.
Lelieveld, J., Haines, A., Pozzer, A., 2018. Age-dependent health risk from ambient air pollution: a modelling and data analysis of childhood mortality in middle-income and low-income countries. The Lancet Planetary Health 2 (7), e292–e300. https://doi.org/10.1016/s2542-5196(18)30147-5.
Lelieveld, J., Pozzer, A., Pöschl, U., Fnais, M., Haines, A., Münzel, T., 2020. Loss of life expectancy from air pollution compared to other risk factors: a worldwide perspective. Cardiovasc. Res. 116 (11), 1910–1917. https://doi.org/10.1093/cvr/cvaa025.
Li, X., Xue, T., Zheng, B., Zhang, Y., 2021. Risk assessment of mortality from acute exposure to ambient fine particles based on the different toxicities of chemical compositions in China. J. Integr. Environ. Sci. 18 (1), 55–66. https://doi.org/10.1080/1943815X.2021.1912106.
Li, M., Zhang, Q., Kurokawa, J.I., Woo, J.H., He, K., Lu, Z., Ohara, T., Song, Y., Streets, D. G., Carmichael, G.R., Cheng, Y., 2017. MIX: a mosaic Asian anthropogenic emission inventory under the international collaboration framework of the MICS-Asia and HTAP. Atmos. Chem. Phys. 17 (2), 935–963. https://doi.org/10.5194/acp-17-935-2017.
Lin, Y., Colle, B.A., 2011. A new bulk microphysical scheme that includes riming intensity and temperature-dependent ice characteristics. Mon. Weather Rev. 139 (3), 1013–1035. https://doi.org/10.1175/2010mwr3293.1.
Liu, M., Huang, X., Song, Y., Xu, T., Wang, S., Wu, Z., Hu, M., Zhang, L., Zhang, Q., Pan, Y., Liu, X., Zhu, T., 2018. Rapid SO 2 emission reductions significantly increase tropospheric ammonia concentrations over the North China Plain. Atmos. Chem. Phys. 18 (24), 17933–17943. https://doi.org/10.5194/acp-18-17933-2018.
Liu, M., Huang, X., Song, Y., Tang, J., Cao, J., Zhang, X., Zhang, Q., Wang, S., Xu, T., Kang, L., Cai, X., 2019. Ammonia emission control in China would mitigate haze pollution and nitrogen deposition, but worsen acid rain. Proc. Natl. Acad. Sci. 116 (16), 7760–7765. https://doi.org/10.1073/pnas.1814880116.
Liu, Z., Zhou, M., Chen, Y., Chen, D., Pan, Y., Song, T., Ji, D., Chen, Q., Zhang, L., 2021. The nonlinear response of fine particulate matter pollution to ammonia emission reductions in North China. Environ. Res. Lett. 16 (3), 034014. https://doi.org/10.1088/1748-9326/abdf86.
Lu, F., Xu, D., Cheng, Y., Dong, S., Guo, C., Jiang, X., Zheng, X., 2015. Systematic review and meta-analysis of the adverse health effects of ambient $PM_{2.5}$ and PM_{10} pollution in the Chinese population. Environ. Res. 136, 196–204. https://doi.org/10.1016/j.envres.2014.06.029.
Maji, K.J., Namdeo, A., Bramwell, L., 2023. Driving factors behind the continuous increase of long-term PM2. 5-attributable health burden in India using the high-resolution global. Sci. Total Environ. 866, 161435. https://doi.org/10.1016/j.scitotenv.2023.161435 datasets from 2001 to 2020.
Metzger, S., Rémy, S., Williams, J.E., Huijnen, V., Flemming, J., 2024. A computationally efficient parameterization of aerosol, cloud and precipitation pH for application at global and regional scale (EQSAM4Clim-v12). Geosci. Model Dev. 17 (12), 5009–5021. https://doi.org/10.5194/gmd-17-5009-2024.
Mitsakou, C., Housiadas, C., Eleftheriadis, K., Vratolis, S., Helmis, C., Asimakopoulos, D., 2007. Lung deposition of fine and ultrafine particles outdoors and indoors during a cooking event and a no activity period. Indoor Air 17 (2). https://doi.org/10.1111/j.1600-0668.2006.00464.x.
Mlawer, E.J., Taubman, S.J., Brown, P.D., Iacono, M.J., Clough, S.A., 1997. Radiative transfer for inhomogeneous atmospheres: RRTM, a validated correlated-k model for the longwave. J. Geophys. Res. Atmos. 102 (D14), 16663–16682. https://doi.org/10.1029/97jd00237.
Oakes, M., Ingall, E.D., Lai, B., Shafer, M.M., Hays, M.D., Liu, Z.G., Russell, A.G., Weber, R.J., 2012. Iron solubility related to particle sulfur content in source emission and ambient fine particles. Environ. Sci. Tech. 46 (12), 6637–6644. https://doi.org/10.1021/es300701c.
Ostro, B., Hu, J., Goldberg, D., Reynolds, P., Hertz, A., Bernstein, L., Kleeman, M.J., 2015. Associations of mortality with long-term exposures to fine and ultrafine particles, species and sources: results from the California Teachers Study Cohort. Environ. Health Perspect. 123 (6), 549–556. https://doi.org/10.1289/ehp.1408565.
Ots, R., Vieno, M., Allan, J.D., Reis, S., Nemitz, E., Young, D.E., Coe, H., Di Marco, C., Detournay, A., Mackenzie, I.A., Green, D.C., 2016a. Model simulations of cooking organic aerosol (COA) over the UK using estimates of emissions based on measurements at two sites in London. Atmospheric Chemistry and Physics 16 (21), 13773–13789. https://doi.org/10.5194/acp-16-13773-2016.
Ots, R., Young, D.E., Vieno, M., Xu, L., Dunmore, R.E., Allan, J.D., Coe, H., Williams, L. R., Herndon, S.C., Ng, N.L., Hamilton, J.F., 2016b. Simulating secondary organic aerosol from missing diesel-related intermediate-volatility organic compound emissions during the Clean Air for London (ClearfLo) campaign. Atmos. Chem. Phys. 16 (10), 6453–6473. https://doi.org/10.5194/acp-16-6453-2016.
Ots, R., Heal, M.R., Young, D.E., Williams, L.R., Allan, J.D., Nemitz, E., Di Marco, C., Detournay, A., Xu, L., Ng, N.L., Coe, H., 2018. Modelling carbonaceous aerosol from residential solid fuel burning with different assumptions for emissions. Atmos. Chem. Phys. 18 (7), 4497–4518. https://doi.org/10.5194/acp-18-4497-2018.
Paerl, H.W., Gardner, W.S., McCarthy, M.J., Peierls, B.L., Wilhelm, S.W., 2014. Algal blooms: noteworthy nitrogen. Science 346 (6206), 175. https://doi.org/10.1126/science.346.6206.175-a.
Pandey, A., Sadavarte, P., Rao, A.B., Venkataraman, C., 2014. Trends in multi-pollutant emissions from a technology-linked inventory for India: II. Residential, agricultural and informal industry sectors. Atmos. Environ. 99, 341–352. https://doi.org/10.1016/j.atmosenv.2014.09.080.
Pandey, A., Brauer, M., Cropper, M.L., Balakrishnan, K., Mathur, P., Dey, S., Turkgulu, B., Kumar, G.A., Khare, M., Beig, G., Gupta, T., 2021. Health and economic impact of air pollution in the states of India: the Global Burden of Disease Study 2019. The Lancet Planetary Health 5 (1), e25–e38. https://doi.org/10.1016/S2542-5196(20)30298-9.
Pawar, P.V., Ghude, S.D., Jena, C., Móring, A., Sutton, M.A., Kulkarni, S., Lal, D.M., Surendran, D., Van Damme, M., Clarisse, L., Coheur, P.-F., Liu, X., Govardhan, G., Xu, W., Jiang, J., Adhya, T.K., 2021. Analysis of atmospheric ammonia over South and East Asia based on the MOZART-4 model and its comparison with satellite and surface observations. Atmos. Chem. Phys. 21, 6389–6409. https://doi.org/10.5194/acp-21-6389-2021.
Pawar, P.V., Ghude, S.D., Govardhan, G., Acharja, P., Kulkarni, R., Kumar, R., Sinha, B., Sinha, V., Jena, C., Gunwani, P., Adhya, T.K., 2023. Chloride (HCl/Cl-) dominates inorganic aerosol formation from ammonia in the Indo-Gangetic Plain during winter: modeling and comparison with observations. Atmos. Chem. Phys. 23 (1), 41–59. https://doi.org/10.5194/acp-23-41-2023.
Pio, C.A. and Harrison, R.M., 1987. Vapour pressure of ammonium chloride aerosol: effect of temperature and humidity. Atmospheric Environment (1967), 21(12), 2711-2715. Doi: 10.1016/0004-6981(87)90203-4.
Pope III, C.A., 2000. Epidemiological basis for particulate air pollution health standards. Aerosol Science & Technology 32 (1), 4–14. https://doi.org/10.1080/027868200303885.
Pope III, C.A., Lefler, J.S., Ezzati, M., Higbee, J.D., Marshall, J.D., Kim, S.Y., Bechle, M., Gilliat, K.S., Vernon, S.E., Robinson, A.L., Burnett, R.T., 2019. Mortality risk and fine particulate air pollution in a large, representative cohort of US adults. Environ. Health Perspect. 127 (7), 077007. https://doi.org/10.1289/ehp4438.
Pope III, C.A., Coleman, N., Pond, Z.A., Burnett, R.T., 2020. Fine particulate air pollution and human mortality: 25+ years of cohort studies. Environ. Res. 183, 108924. https://doi.org/10.1016/j.envres.2019.108924.
Pozzer, A., Tsimpidi, A.P., Karydis, V.A., De Meij, A., Lelieveld, J., 2017. Impact of agricultural emission reductions on fine-particulate matter and public health. Atmospheric Chemistry and Physics 17 (20), 12813–12826. https://doi.org/10.5194/acp-2017-390.
Raizenne, M., Neas, L.M., Damokosh, A.I., Dockery, D.W., Spengler, J.D., Koutrakis, P., Ware, J.H., Speizer, F.E., 1996. Health effects of acid aerosols on North American children: pulmonary function. Environ. Health Perspect. 104 (5), 506–514. https://doi.org/10.1289/ehp.96104506.
Ravishankara, A.R., David, L.M., Pierce, J.R., Venkataraman, C., 2020. Outdoor air pollution in India is not only an urban problem. Proc. Natl. Acad. Sci. 117 (46), 28640–28644. https://doi.org/10.1073/pnas.2007236117.
Robinson, A.L., Donahue, N.M., Shrivastava, M.K., Weitkamp, E.A., Sage, A.M., Grieshop, A.P., Lane, T.E., Pierce, J.R., Pandis, S.N., 2007. Rethinking organic aerosols: Semivolatile emissions and photochemical aging. Science 315 (5816), 1259–1262. https://doi.org/10.1126/science.1133061.
Sadavarte, P., Venkataraman, C., 2014. Trends in multi-pollutant emissions from a technology-linked inventory for India: I. Industry and Transport Sectors. Atmospheric Environment 99, 353–364. https://doi.org/10.1016/j.atmosenv.2014.09.081.
Sang, S., Chu, C., Zhang, T., Chen, H., Yang, X., 2022. The global burden of disease attributable to ambient fine particulate matter in 204 countries and territories, 1990–2019: A systematic analysis of the Global Burden of Disease Study 2019. Ecotoxicol. Environ. Saf. 238, 113588. https://doi.org/10.1016/j.ecoenv.2022.113588.
Sheppard, L.J., Leith, I.D., Mizunuma, T., Neil Cape, J., Crossley, A., Leeson, S., Sutton, M.A., van Dijk, N., Fowler, D., 2011. Dry deposition of ammonia gas drives species change faster than wet deposition of ammonium ions: Evidence from a long-term field manipulation. Glob. Chang. Biol. 17 (12), 3589–3607. https://doi.org/10.1111/j.1365-2486.2011.02478.x.
Simpson, D., Benedictow, A., Berge, H., Bergström, R., Emberson, L.D., Fagerli, H., Flechard, C.R., Hayman, G.D., Gauss, M., Jonson, J.E., Jenkin, M.E., 2012. The EMEP MSC-W chemical transport model–technical description. Atmos. Chem. Phys. 12 (16), 7825–7865. https://doi.org/10.5194/acp-12-7825-2012.
Simpson, D., Andersson, C., Christensen, J.H., Engardt, M., Geels, C., Nyiri, A., Posch, M., Soares, J., Sofiev, M., Wind, P., Langner, J., 2014. Impacts of climate and emission changes on nitrogen deposition in Europe: a multi-model study. Atmos. Chem. Phys. 14 (13), 6995–7017. https://doi.org/10.5194/acp-14-6995-2014.
Simpson, D., Bergström, R., Briolat, A., Imhof, H., Johansson, J., Priestley, M., Valdebenito, A., 2020. GenChem v1. 0–a chemical pre-processing and testing system for atmospheric modelling. Geosci. Model Dev. 13 (12), 6447–6465. https://doi.org/10.5194/gmd-13-6447-2020.
Skamarock, W.C., Klemp, J.B., Dudhia, J., Gill, D.O., Liu, Z., Berner, J., Wang, W., Powers, J.G., Duda, M.G., Barker, D.M. and Huang, X.Y., 2019. A description of the advanced research WRF version 4. NCAR tech. note ncar/tn-556+ str, 145. doi: 10.5065/1dfh-6p97.
Sutton, M.A., Pitcairn, C.E. and Fowler, D., 1993. The exchange of ammonia between the atmosphere and plant communities. In Advances in ecological research (Vol. 24, 301-393). Academic Press.
Sutton, M.A., Howard, C.M., Erisman, J.W., Billen, G., Bleeker, A., Grennfelt, P., Van Grinsven, H. and Grizzetti, B. eds., 2011. The European nitrogen assessment: sources, effects and policy perspectives. Cambridge university press. Doi: 10.1017/CBO9780511976988.
Sutton, M.A., Reis, S., Riddick, S.N., Dragosits, U., Nemitz, E., Theobald, M.R., Tang, Y.S., Braban, C.F., Vieno, M., Dore, A.J., Mitchell, R.F., 2013. Towards a climate-dependent paradigm of ammonia emission and deposition. Philos. Trans. R. Soc., B 368 (1621), 20130166. https://doi.org/10.1098/rstb.2013.0166.
Thunis, P., Crippa, M., Cuvelier, C., Guizzardi, D., de Meij, A., Oreggioni, G., Pisoni, E., 2021. Sensitivity of air quality modelling to different emission inventories: A case

study over Europe. Atmos. Environ.: X 10, 100111. https://doi.org/10.1016/j.aeaoa.2021.100111.
Tomlinson S.J, Carnell E.J, Pearson C., Dragosits U., Jain N., Misselbrook T., and Sutton M.A., A Framework for Gridded Estimates of Ammonia Emissions from Agriculture in South Asia, 2024, Manuscript in preparation.
U.S. Environmental Protection Agency. 2011b. An Overview of Methods for EPA's National-Scale Air Toxics Assessment. Research Triangle Park, NC: U.S. EPA, Office of Air Quality, Planning, and Standards. http://www.epa.gov/ttn/atw/nata2005/05pdf/nata_tmd.pdf.
U.S. Environmental Protection Agency. 2011a. Health Effects Information Used in Cancer and Noncancer Risk Characterization for the 2005 National-Scale Assessment. U.S. EPA, Office of Air and Radiation. Retrieved June 6, 2011a from http://www.epa.gov/ttn/atw/nata2005/05pdf/health_effects.pdf.
U.S. EPA, 2001. Air quality criteria for particulate Matter. Available: https://assessments.epa.gov/isa/document/&deid%3D20810U.S. EPA, 2019. Integrated Science Assessment (ISA) for Particulate Matter EPA/600/R-19/188. Available: https://www.epa.gov/isa/integrated-science-assessment-isa-particulate-matter.
Van Damme, M., Clarisse, L., Heald, C.L., Hurtmans, D., Ngadi, Y., Clerbaux, C., Dolman, A.J., Erisman, J.W., Coheur, P.F., 2014. Global distributions, time series and error characterization of atmospheric ammonia (NH 3) from IASI satellite observations. Atmos. Chem. Phys. 14 (6), 2905–2922. https://doi.org/10.5194/acp-14-2905-2014.
Van Damme, M., Clarisse, L., Whitburn, S., Hadji-Lazaro, J., Hurtmans, D., Clerbaux, C., Coheur, P.F., 2018. Industrial and agricultural ammonia point sources exposed. Nature 564 (7734), 99–103. https://doi.org/10.1038/s41586-018-0747-1.
Van Donkelaar, A., Martin, R.V., Brauer, M., Boys, B.L., 2015. Use of satellite observations for long-term exposure assessment of global concentrations of fine particulate matter. Environ. Health Perspect. 123 (2), 135–143. https://doi.org/10.1289/ehp.1408646.
Venkataraman, C., Brauer, M., Tibrewal, K., Sadavarte, P., Ma, Q., Cohen, A., Chaliyakunnel, S., Frostad, J., Klimont, Z., Martin, R.V. and Millet, D.B., 2018. Source influence on emission pathways and ambient PM 2.5 pollution over India (2015–2050). Atmospheric Chemistry and Physics, 18(11), 8017-8039. Doi: 10.5194/acp-18-8017-2018.
Vieno, M., Heal, M.R., Williams, M.L., Carnell, E.J., Nemitz, E., Stedman, J.R., Reis, S., 2016. The sensitivities of emissions reductions for the mitigation of UK PM 2.5. Atmos. Chem. Phys. 16 (1), 265–276. https://doi.org/10.5194/acp-16-265-2016.
Viscusi, W.K., Masterman, C.J., 2017. Income elasticities and global values of a statistical life. Journal of Benefit-Cost Analysis 8 (2), 226–250. https://doi.org/10.1017/bca.2017.12.
Wang, X., Mauzerall, D.L., 2006. Evaluating impacts of air pollution in China on public health: implications for future air pollution and energy policies. Atmos. Environ. 40 (9), 1706–1721. https://doi.org/10.1016/j.atmosenv.2005.10.066.
Wang, T., Song, Y., Xu, Z., Liu, M., Xu, T., Liao, W., Yin, L., Cai, X., Kang, L., Zhang, H., Zhu, T., 2020a. Why is the Indo-Gangetic Plain the region with the largest NH 3 column in the globe during pre-monsoon and monsoon seasons? Atmos. Chem. Phys. 20 (14), 8727–8736. https://doi.org/10.5194/acp-20-8727-2020.
Wang, Y., Wild, O., Chen, H., Gao, M., Wu, Q., Qi, Y., Chen, X., Wang, Z., 2020b. Acute and chronic health impacts of PM2. 5 in China and the influence of interannual meteorological variability. Atmos. Environ. 229, 117397. https://doi.org/10.1016/j.atmosenv.2020.117397.
Warner, J.X., Dickerson, R.R., Wei, Z., Strow, L.L., Wang, Y., Liang, Q., 2017. Increased atmospheric ammonia over the world's major agricultural areas detected from space. Geophys. Res. Lett. 44 (6), 2875–2884. https://doi.org/10.1002/2016gl072305.
Watanabe, K.H., Djordjevic, M.V., Stellman, S.D., Toccalino, P.L., Austin, D.F., Pankow, J.F., 2009. Incremental lifetime cancer risks computed for benzo [a] pyrene and two tobacco-specific N-nitrosamines in mainstream cigarette smoke compared with lung cancer risks derived from epidemiologic data. Regul. Toxicol. Pharm. 55 (2), 123–133.
Weber, R.J., Guo, H., Russell, A.G., Nenes, A., 2016. High aerosol acidity despite declining atmospheric sulfate concentrations over the past 15 years. Nat. Geosci. 9 (4), 282–285. https://doi.org/10.1038/ngeo2665.
Whaley, C.H., Law, K.S., Hjorth, J.L., Skov, H., Arnold, S.R., Langner, J., Pernov, J.B., Bergeron, G., Bourgeois, I., Christensen, J.H., Chien, R.Y., 2023. Arctic tropospheric ozone: assessment of current knowledge and model performance. Atmos. Chem. Phys. 23 (1), 637–661. https://doi.org/10.5194/acp-2022-319.
WHO, 2018. WHO Global Urban Ambient Air Pollution Database (Update 2018). Available: .
WHO, 2021. Global air quality guidelines: particulate matter (PM2.5 and PM10), ozone, nitrogen dioxide, sulfur dioxide and carbon monoxide. Available: https://www.who.int/publications/i/item/9789240034228.
Wiedinmyer, C., Akagi, S.K., Yokelson, R.J., Emmons, L.K., Al-Saadi, J.A., Orlando, J.J., Soja, A.J., 2011. The Fire INventory from NCAR (FINN): A high resolution global model to estimate the emissions from open burning. Geosci. Model Dev. 4 (3), 625–641. https://doi.org/10.5194/gmd-4-625-2011.
World bank Institute for health Metrics and Evaluation, "The cost of air pollution Strengthening the economic case for action" (World bank, 2016).
World Bank, 2023. Striving for Clean Air: Air Pollution and Public Health in South Asia. Available: https://www.worldbank.org/en/region/sar/publication/striving-for-clean-air.
Xu, Z., Liu, M., Zhang, M., Song, Y., Wang, S., Zhang, L., Xu, T., Wang, T., Yan, C., Zhou, T., Sun, Y., 2019. High efficiency of livestock ammonia emission controls in alleviating particulate nitrate during a severe winter haze episode in northern China. Atmos. Chem. Phys. 19 (8), 5605–5613. https://doi.org/10.5194/acp-19-5605-2019.
Zhang, Y., Dore, A.J., Ma, L., Liu, X.J., Ma, W.Q., Cape, J.N., Zhang, F.S., 2010. Agricultural ammonia emissions inventory and spatial distribution in the North China Plain. Environ. Pollut. 158 (2), 490–501. https://doi.org/10.1016/j.envpol.2009.08.033.
Zhang, Q., Zheng, Y., Tong, D., Shao, M., Wang, S., Zhang, Y., Xu, X., Wang, J., He, H., Liu, W. and Ding, Y., 2019. Drivers of improved PM2. 5 air quality in China from 2013 to 2017. Proceedings of the National Academy of Sciences, 116(49), 24463-24469. Doi: 10.1073/pnas.1907956116.
Zwozdziak, A., Gini, M.I., Samek, L., Rogula-Kozlowska, W., Sowka, I., Eleftheriadis, K., 2017. Implications of the aerosol size distribution modal structure of trace and major elements on human exposure, inhaled dose and relevance to the PM2. 5 and PM10 metrics in a European pollution hotspot urban area. J. Aerosol Sci 103, 38–52. https://doi.org/10.1016/j.jaerosci.2016.10.004.